Accepted Manuscript

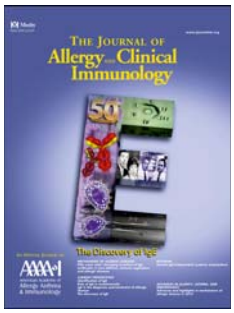

TLR7/8 agonists stimulate plasmacytoid dendritic cells to initiate a Th17-deviated acute contact dermatitis in humans

Natalie Garzorz-Stark, MD, PhD, Felix Lauffer, MD, Linda Krause, PhD, Jenny Thomas, PhD, Anne Atenhan, Regina Franz, MD, Sophie Roenneberg, MD, Alexander Boehner, MD, Manja Jargosch, PhD, Richa Batra, PhD, Nikola S. Mueller, PhD, Stefan Haak, PhD, Christina Groß, PhD, Olaf Groß, PhD, Claudia Traidl-Hoffmann, MD, Fabian J. Theis, PhD, Carsten B. Schmidt-Weber, PhD, Tilo Biedermann, MD, Stefanie Eyerich, PhD, Kilian Eyerich, MD, PhD

PII: S0091-6749(17)31442-2

DOI: 10.1016/j.jaci.2017.07.045

Reference: YMAI 13009

To appear in: *Journal of Allergy and Clinical Immunology*

Received Date: 13 March 2017

Revised Date: 8 June 2017

Accepted Date: 24 July 2017

Please cite this article as: Garzorz-Stark N, Lauffer F, Krause L, Thomas J, Atenhan A, Franz R, Roenneberg S, Boehner A, Jargosch M, Batra R, Mueller NS, Haak S, Groß C, Groß O, Traidl-Hoffmann C, Theis FJ, Schmidt-Weber CB, Biedermann T, Eyerich S, Eyerich K, TLR7/8 agonists stimulate plasmacytoid dendritic cells to initiate a Th17-deviated acute contact dermatitis in humans, *Journal of Allergy and Clinical Immunology* (2017), doi: 10.1016/j.jaci.2017.07.045.

TLR7/8 agonists stimulate plasmacytoid dendritic cells to initiate a Th17-deviated acute contact dermatitis in humans

Natalie Garzorz-Stark, MD, PhD[1,†,*], Felix Lauffer, MD[†,1], Linda Krause, PhD[2], Jenny Thomas, PhD[3], Anne Atenhan[3], Regina Franz, MD[1], Sophie Roenneberg, MD[1], Alexander Boehner, MD[1], Manja Jargosch, PhD[3], Richa Batra, PhD[2], Nikola S. Mueller, PhD[2], Stefan Haak, PhD[3], Christina Groß, PhD[4], Olaf Groß, PhD[4], Claudia Traidl-Hoffmann, MD[5], Fabian J. Theis, PhD[2,6], Carsten B Schmidt-Weber, PhD[3], Tilo Biedermann, MD[1], Stefanie Eyerich, PhD[3, ††], Kilian Eyerich, MD, PhD[1, ††]

Affiliations

[1] Department of Dermatology and Allergy, Technical University of Munich, Munich, Germany

[2] Institute of Computational Biology, Helmholtz Center Munich, Neuherberg, Germany, Member of the German Center for Lung Research (DZL)

[3] ZAUM – Center of Allergy and Environment, Technical University and Helmholtz Center Munich, Munich, Germany, Member of the German Center for Lung Research (DZL)

[4] Institute for Clinical Chemistry and Pathobiochemistry, Technical University of Munich, Munich, Germany

[5] Chair and Institute of Environmental Medicine UNIKAT, Technical University and Helmholtz Center Munich, Augsburg, Germany

[6] Department of Mathematics, Technical University of Munich, Garching, Germany

[†] N.G. and F.L. contributed equally to this work

[†] S.E. and K.E. contributed equally to this work

Corresponding author

To whom correspondence should be addressed: Natalie Garzorz, MD, PhD, Department of Dermatology and Allergy, Biedersteiner Strasse 29, 80802 Munich, Germany; fon: +49-89-41403195; fax: +49-89-41403453; mail: natalie.garzorz@tum.de

Sources of funding

This work was supported by the European Research Council (IMCIS 676858 and FLAMMASEC 337689), German Research Foundation (EY97/3-1), the Bavarian Molecular Bio- systems Research Network (BioSysNet), and the Helmholtz Association ("Impuls- und Vernetzungsfonds"). L.K. is supported by the German Research Foundation (DFG) through the Graduate School of Quantitative Biosciences Munich.

Abstract

Background: A standardized human model to study early pathogenic events in psoriasis is missing. Activation of Toll-like receptor 7/8 by topical application of imiquimod is the most commonly used mouse model of psoriasis.

Objective: To investigate the potential of a human imiquimod patch test model to resemble human psoriasis.

Methods: Imiquimod (Aldara® 5% cream) was applied twice a week onto the back of volunteers (n=18) and the development of skin lesions was monitored over a time period of four weeks. Consecutive biopsies were taken for whole genome expression analysis, histology and T cell isolation. pDC were isolated from whole blood, stimulated with TLR7 agonist and analysed by extracellular flux analysis and real time PCR.

Results: We demonstrate imiquimod induces a monomorphic and self-limited inflammatory response in healthy individuals as well as psoriasis or eczema patients, respectively. The clinical and histologic phenotype as well as transcriptome of imiquimod-induced inflammation in human skin resembles an acute contact dermatitis rather than psoriasis. Nevertheless, the imiquimod model mimics hallmarks of psoriasis. Namely, plasmacytoid dendritic cells (pDC) are primary sensors of imiquimod, responding with production of pro-inflammatory and Th17-skewing cytokines. This results in a Th17 immune response with IL-23 as a key driver. In a *proof-of-concept* setting, systemic treatment with ustekinumab diminished the imiquimod-induced inflammation.

Conclusion: In humans, imiquimod induces contact dermatitis with the distinctive feature that pDC are the primary sensors, leading to an IL-23/Th17 deviation. Despite these shortcomings, the human imiquimod model might be useful to investigate early pathogenic events and prove molecular concepts in psoriasis.

Key messages

- Epicutaneous application of imiquimod in humans induces a self-limited contact dermatitis-like reaction with signs of cytotoxicity and cell stress.
- This reaction is initiated by plasmacytoid dendritic cells and shows a deviation towards the IL-23/Th17 axis – the typical molecular signature of human psoriasis.
- The imiquimod model in humans represents a limited model of the molecular signature of psoriasis.

Capsule summary

Stimulation of TLR7/8 in human skin induces an acute contact dermatitis with pDC as primary sensors and IL-23 as essential driver of the reaction, thus constituting a standardized, but limited model of human psoriasis.

Key words

Psoriasis, contact dermatitis, Imiquimod, Aldara, plasmacytoid dendritic cell, IL-23, Th17, cytotoxicity, Toll-like receptor, innate immunity

Abbreviations

ACD	Allergic contact dermatitis

76	ICD	Imiquimod-induced contact dermatitis
77	IFN	Interferon
78	IL	Interleukin
79	pDC	plasmacytoid dendritic cell
80	Th	T helper cell
81	TNF	Tumor necrosis factor
82	TLR	Toll like receptor

Introduction

Psoriasis is a non-communicable inflammatory skin disease classified by the World Health Organization as severe disease. Despite enormous efforts, psoriasis is still underdiagnosed and undertreated [1]. One reason for these shortcomings is the remarkable heterogeneity in the clinical spectrum of psoriasis [2]. This heterogeneity is reflected by a high inter-individual as well as inter-investigational variability in the transcriptome of psoriasis plaques [3-5]. Using meta-analysis approaches, downstream core-genes expressed in most psoriasis plaques were proposed [6, 7]. While these downstream genes represent targets of highly efficient biologic therapies, identification of early psoriasis triggers remains difficult. At the same time, murine models only partially reflect human psoriasis [8, 9]. Thus, there is a high need to identify a human model that allows the standardized investigation of psoriasis plaque formation and kinetics.

Epicutaneous application of the Toll-like-receptor (TLR) 7/8 agonist imiquimod is regarded the most widely used model for psoriasis in mice [10]. Daily application of imiquimod results in a self-limited, localized cutaneous immune response resembling histological hallmarks of psoriasis such as parakeratosis, acanthosis, and neutrophil microabscesses in mice [11]. Furthermore, molecular pathways central in human psoriasis are upregulated upon imiquimod-stimulation, among them IFN-γ, TNF-α, and the IL-23/Th17 axis [12-14]. While it remains unclear what exactly drives the imiquimod-induced psoriasis-like skin inflammation in mice, dendritic cells and γδT cells are indispensable for its development [15, 16]. In humans, incidental exacerbation of a pre-existing psoriasis plaque in a psoriasis patient after application of imiquimod is reported [17], and a case series reports skin lesions partially reflecting human psoriasis after short-term application of imiquimod [12].

The aim of this study was to comprehensively characterize the imiquimod-induced inflammation in humans and to evaluate its potential use as a standardized human psoriasis model.

Materials and methods

Patient characteristics and study design

18 patients with or without known history of psoriasis, atopic eczema, or both, were included into the study (Table 1). The study was conducted according to the declaration of Helsinki and approved by the local ethics committee (5060/11). 0.2g/cm² Imiquimod (Aldara® 5% cream) was applied at day 0, 2, 4, and subsequently twice weekly for 4 weeks in an occlusive manner at the back of the patients. Systemic immune-suppressive treatments for three months or topical immune-suppressive treatment one week prior to inclusion into the study were exclusion criteria.

Punch biopsy specimens

6mm punch biopsies were obtained under local anaesthesia after written informed consent was obtained. Punch biopsies were cut into three pieces – one third was paraffin-embedded for histological assessment, total RNA was isolated from the second third, and primary human cells were obtained from the last piece.

Histology

Histology assessment was performed by two independent blinded pathologists. To evaluate histological similarity to psoriasis or eczema, samples were scored according to a published psoriasis and eczema score [12]. Each criterion was evaluated separately: Absence of a characteristic was evaluated with 0 point, mild presence of the characteristic with 1 point and full presence of the characteristic with 2 points. Thus, a maximum of 16 points could be achieved for the psoriasis score and a maximum of 12 points for the eczema score.

Immune-histochemistry

Skin samples were fixed in 10% formalin and embedded in paraffin. 4 µm sections were cut and dewaxed. Stainings were performed by an automated BOND system according to the manufacturer's instructions: After rehydration and antigen retrieval in a pH 6 citrate buffer based epitope retrieval solution (Leica), sections were incubated with the monoclonal antibodies rabbit anti-CD4 (Zytomed Systems) and mouse anti-CD8 (Zytomed Systems), goat anti-IL-17 (R&D Systems), rabbit anti-

neutrophil elastase (Abcam), rabbit anti-TLR7 (Abcam), Caspase 3 (Cell Signalling), mouse anti-CD303 (Dendritics) antibodies. Secondary polymeric alkaline phosphatase (AP)-linked anti-rabbit antibody and horseradish peroxidase (HRP)-linked anti-mouse antibody (Zytomed Systems) were applied and the complex was visualized by the substrate chromogen Fast Red or 3,3'-diaminobenzidine (DAB). For goat anti-IL-17 a goat bridge (Polyclonal goat anti-IL-17 antibody, R&D Systems) was applied before application of the secondary antibody. Eventually, slides were counterstained with haematoxylin. As a negative control, primary antibodies were omitted or replaced with an irrelevant isotype-matched monoclonal antibody. Positive cells of each slide were counted in two visual fields (400x) per condition by two independent investigators in a blinded manner.

Immune-fluorescence

Paraffin mounted slides were dewaxed and rehydrated in consecutive washes with Roticlear (two changes à 10 min), followed by isopropanol (two changes à 5 min), 96% and 70% ethanol (one change à 5 min, respectively) and dH_2O (one change à 5 min). Antigen retrieval was performed in a pressure cooker with boiling citrate buffer (approx. 96°C) for 7 minutes followed by a washing step with Tris buffer and a blocking step with peroxidase 3% for 15 minutes sections at room temperature (RT). Before applying the primary antibody (anti-iNOS antibody, Novus Biologicals) for 1h at RT and then overnight, sections were washed with Tris buffer and blocked with 10% normal goat serum and 10% normal donkey serum for 1h. After overnight incubation, slides were rinsed with Tris buffer and incubated with secondary antibody (488 goat-anti rabbit antibody, Life Technologies) in the dark for 1h at RT. After rinsing with Tris buffer, sections were incubated in 0.1% Sudan Black B, diluted in 70% ethanol followed by a washing step with 0.02% Tween 20 diluted in PBS and several changes of dH_2O. Before mounting the sections in Vectashield Mounting Medium, incubation with DAPI for two minutes was performed. Then, images in the blue (DAPI) and green (iNOS) channel of an Olympus IX73 inverted fluorescence microscope were taken.

Isolation and stimulation of lesional T cells

T cells were isolated from freshly taken skin biopsies. Samples were placed in 24-well plates – pre-coated with α-CD3 (0.75 µg/ml α-CD3) for 1 h - containing T cell culture medium, 0.75 µg/ml α-

CD28 and 60 U/ml IL-2 and incubated at 37°C, 5% CO_2. Fresh medium containing 60 U/ml IL-2 was replaced three times a week and T cells emigrated from tissue samples were expanded and harvested for flow cytometry. For protein secretion analysis, supernatant from T cells that were stimulated with plate-bound α-CD3 and soluble α-CD28 (both 0.75 µg/ml) was obtained and analysed with the Human Cytokine 27-Plex Assay according to the manufacturer's recommendation (Bio-Rad).

Isolation and stimulation of human pDC

Human pDC were isolated using the Plasmacytoid Dendritic Cell Isolation II (Miltenyi Biotech) from peripheral blood mononuclear cells leaving a pure and untouched pDC fraction. pDC were stimulated with Imiquimod, R848 and Gardiquimod (100µM each) for 6 hours in RPMI supplemented with 1% human serum, 2mM glutamine, 1mM sodium pyruvate, 1% non-essential amino acids and 1% penicillin/streptomycin.

Flow cytometry

For surface staining of T cells, the following antibodies were used: CD4 labeled with HorizonV500 or APC-Cy7, CD8 labeled with Fitc, Pacific Blue or APC-Cy7 (all BD Biosciences). For intracellular staining, T cells were stimulated with 10ng/ml PMA, 1µg/ml Ionomycin and GolgiStop (BD Biosciences) according to the manufacturer's recommendation for 2 hours. GolgiPlug (BD Biosciences) was added for the last 4 hours of culture. Cells were fixed and permeabilized with Cytofix/Cytoperm solution (BD Biosciences) prior to intracellular staining with the following antibodies: IFN-γ labeled with Fitc or HorizonV450, IL-17 Pe (all BD Biosciences), IL-22 labeled with APC or eF660 (both eBioscience). Cells were analyzed with the LSRFortessa flow cytometer (BD Biosciences) and FlowJo. All gates were set according to isotype controls.

Extracellular Flux Analysis

Human and murine pDCs were resuspended in bicarbonate- and phenol red-free DMEM containing 10 mM glucose, 2 mM glutamine, 1 mM pyruvate and 1% FCS (Sigma-Aldrich), and seeded in 96-well Seahorse plates (Agilent) at a density of 0.15×10^6 cells/well. Cells were incubated at 37°C in a CO_2-free incubator for 1 hour prior to the experiment. Oxygen consumption and extracellular acidification

were measured using a Seahorse XF96 Extracellular Flux Analyzer (Agilent). The compounds (Imiquimod, R848 and Gardiquimod) as well as Rotenone (2µm) to block complex 1 were added at the indicated time points.

RT-PCR

For amplification of genes of interest, first cDNA was synthesized from 500 ng total RNA and transcribed using the High Capacity cDNA Reverse Transcript Amplification Kit (Applied Biosystems) according to the manufacturer's protocol. Primers amplifying genes of interest were designed using the publicly accessible Primer3 software (http://frodo.wi.mit.edu/primer3/). Real time PCR reactions were performed in 384-well plates using the Fast Start SYBR Green Master mix (Roche Applied Science) and fluorescence development was monitored using the ViiA7 Real Time PCR machine (Applied Biosystems). The expression of transcripts was normalized to expression of 18S ribosomal RNA as housekeeping gene. Data were expressed as fold change, relative to unstimulated cells as calibrator. Relative quantification was determined according to the formula: $(RQ) = 2^{-ddCt}$.

Primers used: 18S fw: GTA ACC CGT TGA ACC CCA TT rev: CCA TCC AAT CGG TAG TAG CG; IL-36G fw: AGGAAGGGCCGTCTATCAATC rev: CACTGTCACTTCGTGGAACTG; IL1-ß fw: AAGCCCTTGCTGTAGTGGTG rev: GAAGCTGATGGCCCTAAACA; IFN-α fw: CTTGACTTGCAGCTGAGCAC rev: CAGAGTCACCCATCTCAGCA; IL-23 fw: CTCAGGGACAACAGTCAGTTC rev: ACAGGGCTATCAGGGAGCA; TNF-α fw: GCCAGAGGGCTGATTAGAGA rev: TCAGCCTCTTCTCCTTCCTG; IL-6 fw: GTCAGGGGTGGTTATTGCAT rev: AGTGAGGAACAAGCCAGAGC

Isolation of total RNA from skin

Total RNA was isolated with the miRNeasy Mini Kit according to the manufacturer's protocol. The RNA yield and quality was determined with a Nanodrop ND1000 UV-vis Spectrophotomer. Moreover, the RNA integrity numbers (RIN) were measured using the 2100 Bioanalyzer (Agilent) according to the manufacturer's protocol (Agilent RNA 6000 Nano Kit). RNA samples with RIN>6 were Cy3 labelled, amplified and hybridized on SurePrint G3 Human GE 8x60K BeadChips (Agilent

Technologies). Fluorescence signals were detected with the iScan microarray scanner and extracted using the Agilent Feature Extraction Software (Agilent Technologies). Transcriptome data from psoriasis (n=24) and ICD (n=10) samples were previously published [3] and uploaded to the GEO database (accession number GSE57225).

Preprocessing of whole genome expression data

For statistical analysis of microarray data, R software (http://www.r-project.org) and the limma package from Bioconductor (http://www.bioconductor.org) were used for reading the arrays. Then QualityMetrics for quality control of arrays from Bioconductor was applied. Data was background-corrected using the "normexp" method (also from limma package) and then normalized between the arrays by the "quantile" method (from limma package). Control probes and low expressed probes with normalized signal intensities less than 10% of the 95th percentile of the negative controls of each array were filtered out. Within-array replicates for each probe were averaged by using avereps (from limma package). Then “blastn” (https://blast.ncbi.nlm.nih.gov/Blast.cgi?PAGE_TYPE=BlastSearch) was used to map the 60-basepairs-long nucleotide sequences from the array (= probes) to the UCSC release of the human transcriptome available as RefSeqIDs. Only 100% accurate mappings were considered and saved. Out of all probes, 13,430 did not match with 100% accuracy to a position of the human transcriptome. Probes mapping to two different RefSeq IDs were checked if they corresponded to the same gene (via Gene Symbol). The genes corresponding to the RefSeqID were received via the AnnotationDbi (from Bioconductor) that used the org.Hs.eg.db annotation Package. Eventually, 2,229 probes had to be taken out from analysis because the mapped to several genes. In total, 26,664 probes mapped with 100% accuracy to a unique gene.

Whole genome expression vizualization

Whole genome vizualization was calculated on normalized 26,664 probes for all samples using AC-PCA. This method performs dimension reduction and adjustes for confounding factors at the same time. We used the different patients as confounding factors to correct for inter-individual heterogeneity. For better between-group comparison, 95% confidence intervals per groups were calculated and plotted.

Statistical modeling of gene expression data

The surrogate variable analysis (sva) from Bioconductor was used to estimate artifacts from microarray data. One surrogate variable for the data set was calculated and we included this variable as a covariate in our regression model. Using the "lme4" package of the R software (https://cran.r-project.org/web/packages/lme4/index.html), a linear mixed-effects (LMM) model was fitted to the data with the REML (restricted maximum likelihood) criterion by using one model per probe. The different patients were included as random effects (= random intercepts). Thus, the gene expression level for each patient was adjusted individually. The estimated coefficients from these models are comparable to fold changes or fold inductions. P values for the coefficients were calculated using the mixed function from the "afex" package of the R software (https://cran.r-project.org/web/packages/afex/index.html) which applies the Kenward-Roger approximation for the degrees of freedom. P values were adjusted for multiple testing by Bonferroni correction. Genes were defined as significant when the adjusted p value was below 0.05 and top hits were defined when the absolute fold change was > 2.5.

Gene network analysis

Pathways upregulated in ICD, ACD and psoriasis were analyzed by the ConsensusPathDB database (http://consensuspathdb.org/). Here, using the "Over-representation analysis" tool, pathways from the pathway databases PID, reactome and Biocarta were selected (selection criteria: minimum overlap with input list=2 and p value cutoff=0.01). Among the enriched pathway-based sets, the interaction of pathways for ICD was visualized in a network. For reasons of clarity, only those pathways fulfilling furthermore the criteria minimum overlap=10, presence of at least 30% of genes within the given pathway and a maximum gene set size of each pathway=150 were displayed in the network. Besides, redundant pathways sharing more than 85% together with another given pathway were also taken out from the network. Networks data integration was performed using Cytoscape 3.4.0 software (www.cytoscape.org).

Further statistical analysis

Statistical differences in ICD versus psoriasis, ACD, or eczema lesions, respectively, regarding immune-histochemistry, flow cytometry, and luminex readouts were tested using the Kruskal-Wallis Test.

Polyserial correlation was computed to show the association of clinical severity with the expression levels of BDCA-2 or TLR7, respectively. R package polycor was used. ANOVA and a post-hoc Tukey's test was applied for pairwise analysis among the severity levels using R package stats.

Results

TLR7/8 stimulation results in a self-limited contact dermatitis-like reaction in humans

Topical application of imiquimod (Aldara® 5% cream) at non-lesional skin over a period of 28 days induced skin lesions resembling the clinical course of an acute contact dermatitis. Initially, an erythema was observed, followed by papules and induration, and finally erosions and crusts appeared (Figure 1A). The intensity of response was heterogeneous, with 5/18 patients only reacting with mild erythema, 2/18 with erythema and papules, and 11/18 with the full clinical picture including erosions (Table 1). The clinical reaction to imiquimod did not augment with repetitive application in all patients. 9/18 patients showed a maximum reaction at day 4, 3/18 at day 14, and 6/18 patients at day 28 (Table 1). Among the healthy volunteers, psoriasis, or atopic eczema patients, neither maximum intensity nor kinetics of the reaction were related to the disease background (Table 1). After withdrawal of imiquimod, lesions were self-limited within 30 days (Figure 1A). Application of vehicle (Aldara® cream not containing imiquimod) did not result in a clinical reaction in one exemplatory patient (Figure S1).

Blinded histopathology assessment of punch biopsies resulted in the diagnosis of acute dermatitis in all specimens (n=44 biopsies of the 18 participants, Table 1), with clear signs of spongiosis and eventually serum crusts soaked by neutrophil granulocytes (Figure 1B). In 10/18 patients, infiltrates deeply penetrating into dermal tissue were observed at one or more time points (Figure 1B). Hallmarks of psoriasis such as regular acanthosis, parakeratosis, loss of stratum granulosum, and micro-abscesses were absent in all samples. To quantify the similarity of the imiquimod-induced contact dermatitis (ICD, n=16) with both psoriasis and eczema, respectively, histopathological scores [12] were determined for biopsy sections of psoriasis (n=14), eczema (n=12), and study participants before (n=12) application of imiquimod (Figure 1C). Results confirmed a low similarity of ICD to psoriasis in the psoriasis score (ICD: 2.81+/-0.68; psoriasis: 11.14+/-0.79) and higher values in the eczema score (ICD: 6.69+/- 0.43; psoriasis: 1.86 +/-0.35) for ICD.

The transcriptome of human imiquimod-induced dermatitis closely overlaps with contact dermatitis, but also shares pathways with psoriasis

To investigate the imiquimod-induced contact dermatitis (ICD) in a heuristic global approach, whole genome expression analysis of lesional skin (n=16) was compared to psoriasis (n=24), allergic contact dermatitis to nickel (n=10), eczema (n=15), and non-involved skin (n=26). In a first step, a dimension reduction simultaneously adjusting for the confounding variation from patient heterogeneity was performed (AC-PCA) [18]. A close overlap of ICD with both ACD and psoriasis reactions as compared to non-involved skin was observed when looking at the 95% confidence intervals per group (Figure 2A).

To get a more detailed insight into similarity of ICD and psoriasis, ACD, or eczema, respectively, significantly regulated genes were compared. ICD and ACD transcriptome showed a strong correlation of all significantly regulated genes (r=0.78). In comparison, ICD and psoriasis (r=0.57) as well as ICD and eczema (r=0.56) correlated less (Figure 2B, Figure S2A). Furthermore, 65% of all significantly regulated genes in ACD were also regulated in ICD, while 31.2% of the psoriasis and 37.1% of the eczema genes were also regulated in ICD (Figure 2C, Figure S2B). Among the top hit genes with a log2 fold induction of >2.5, the overlap was higher, with 80.2%, 41.8%, and 64.3% for the ACD, psoriasis, and eczema transcriptome, respectively (Figure 2C, Figure S2B).

ICD is dominated by a cytotoxic T cell response – similarities to ACD, but not to psoriasis

To investigate similarities and differences of ICD (n=16) as compared to psoriasis (n=24) or ACD (n=10) in a qualitative manner, gene network analysis of common and unique pathways were investigated (Table S1, Figure S3). ICD and ACD showed a strong correlation in regulated genes related to apoptosis (r=0.89). Correlation of ICD and psoriasis was less remarkable (r=0.61, Figure 3A, Figure S5).

In line with the latter observation, immune-histochemical stainings showed that more cytotoxic CD8+ T cells infiltrated ICD lesions (89.3+/-12.58, n=16) than psoriasis (42.3+/-7.97, n=11; p=0.0008). No

significant difference was found comparing the number of CD8+ T cells infiltrating ICD and ACD (64.8+/-12.05, n=6); (Figure 3B, Figure S4). Accordingly, the ratio of CD4/CD8 T cells was lower in ICD as compared to ACD, psoriasis, and eczema (Figure 3C, Figure S2B).

Isolation of T cells from lesional skin confirmed a higher frequency of CD8+ T cells than CD4+ T cells in ICD (55.7+/-5.79% versus 27.6+/-6.63%, n=10) as compared to psoriasis (44.8+/-7.5%, versus 38.8+/-7.23%, n=14) (Figure 3D). Differences to ACD were less pronounced (50.8+/-13.38% versus 36.4+/-18.17%, n=7). The ratio of CD4/CD8 T cells was lower in cells investigated *in vitro* as compared to immunehistochemical stainings. A substantial population of both CD4+ and CD8+ T cells secreted Interferon-γ (IFN-γ) as investigated by intracellular cytokine staining (Figure 3D). While a substantial frequency of CD8+ and CD4+T cells in ICD produced IFN-γ (61.4+/-6.41% versus 56.8+/-6.93%, n=10), the frequencies of IFN-γ+ cells were comparable in psoriasis and ACD (CD8+ 43.0+/-4.60%, n=14, CD4+ 29.6+/-5.11% and CD8+ 48.3+/-3.24%, CD4+ 29.8+/-10.81%, n=7, respectively). However, T cells isolated from ICD secreted more IFN-γ upon T cell receptor stimulation (23618+/-1487pg/ml, n=10) than T cells from psoriasis (3167+/-774 pg/ml, n=12) or ACD (2988+/-1062 pg/ml, n=8), respectively (Figure 3E). No significant differences in secretion of CXCL-10 was detectable (Figure 3E).

To assess the functional consequence of this cytotoxic T cellular infiltrate in ICD, the level of caspase 3+ cells was quantified *in situ* (Figure 3F). ICD contained more caspase 3+ cells (6.9+/-1.30 per visual field, n=6) than ACD (4.1+/-0.57, n=9). This is consistent with the gene network analysis revealing more programmed cell death and caspase related pathways in ICD than in ACD. Caspase 3+ cells were very low in psoriasis (1.3+/-0.46, n=6).

In contrast to ACD reactions, pDC are the primary responder cells in ICD

We next assessed whether the primary target of imiquimod would explain differences to ACD. Gene network analysis of pathways unique for ICD identified interferon-signalling to be regulated exclusively in ICD (Figure 4A, Figure S3). 53/73 genes related to the signalling pathway "interferon-

alpha/beta signalling" were significantly regulated in ICD, while only 12/73 were regulated in psoriasis and 13/73 in ACD (Figure S7). As TLR7/8 are highly expressed by plasmacytoid dendritic cells (pDC) and pDC are main producers of IFN-α, pDC were investigated in ICD reactions.

In situ stainings of pDC using the marker BDCA2 demonstrated higher numbers of pDC in ICD (18.0+/-3.69, n=16) than in psoriasis (5.2+/-2.13, n=12) or ACD (14.8+/-3.49, n=6; Figure 4B, Figure S6). The main receptor for imiquimod, TLR7, increased during the clinical course of the ICD reaction as compared to non-involved skin (Figure 4B). Likewise, the number of BDCA2+ cells increased, pointing towards an influx of pDC and upregulation of the receptor upon ligation *in situ* (Figure 4B). Immunehistochemical double staining identified numerous BDCA2+TLR7+ cells (Figure S6). The severity of the clinical reaction correlated with the number of BDCA2+ cells (r^2=0.610) and TLR7 density (r^2= 0.505), indicating a functional role for pDC in ICD (Figure 4C).

Stimulation of pDC with imiquimod resulted in a decrease in mitochondrial respiration and increase in glycolytic extracellular acidification in extracellular flux analysis (Figure 4D). Of note, this was not observed upon pDC stimulation with further TLR7/8 agonists such as R848 or gardiquimod, confirming a TLR7/8 independent metabolic reprogramming activating the NLRP3 inflammasome by imiquimod [19]. This reprogramming by imiquimod was observed both in human pDC (Figure 4D) and in murine pDC (Figure S8), indicating a shared cellular mechanism between mouse imiquimod induced psoriasis like reaction and ICD. Ligation of TLR7/8 by imiquimod, R848 and gardiquimod, respectively, stimulated pDC to produce pro-inflammatory and Th17-associated molecules, among them: IL-1β (mean fold induction by imiquimod/ R848/ gardiquimod: 111/ 47/ 106), IL-6 (403/ 132/ 317), IL-23 (73/ 15/ 25), IL-36G (316/ 314/ 59), IFN-γ (69/ 7021/ 2), TNF-α (70/ 184/ 108), and CXCL8 (1885/ 246/ 131) as compared to non-stimulated control pDC (n=3 different donors; Figure 4E).

pDC induce the IL-23/Th17 axis and influx of neutrophils in ICD

Since pDC are involved in the early pathogenesis of psoriasis, we next investigated the molecular overlap of ICD and psoriasis. Gene network analysis identified IL-23 mediated signalling events as a key pathway upregulated in both ICD and psoriasis (Figure 5A, Figure S3). 21/42 genes related to the IL-23 signalling pathway were significantly regulated in ICD. IL-23A was significantly upregulated in both ICD and psoriasis, but not in ACD, respectively (Figure 5B, Figure S9). IL-23 is a key driver of Th17 immunity. Accordingly, IL-17+ cells were more frequent in ICD (10.3+/-1.78, n=16) than in ACD (4.0+/-0.83, n=8), and comparable to psoriasis *in situ* (9.2+/-1.88, n=13; Figure 5C, D). Immune-histochemical findings were confirmed *in vitro*. 16.6+/-6.04% of T cells isolated from ICD lesions (n=10) produced IL-17 in ICD as compared to psoriasis (9.5+/-3.65%) and ACD (10.1+/-3.29%). IL-22+ cells were reduced in ICD (7.3+/-2.22%) compared to ACD (16.1+/-4.90%) and psoriasis (13.9+/-3.91%) (Figure 5E). Likewise, ICD-derived T cells secreted high amounts of IL-17 after TCR stimulation *in vitro* (13408+/-9139 pg/ml, n=10) as compared to ACD (1612+/-704 pg/ml, n=8) and even psoriasis (2677+/-1057pg/ml, n=12; Figure 5F).

Besides IL-17, T cells derived from ICD also secreted significantly higher amounts of IL-6 (1012+/-80pg/ml, n=10), a cytokine involved in Th17 cell differentiation, than ACD (113+/-63pg/ml, n=8; p=0.0007) or psoriasis (433+/-236pg/ml, n=12; p=0.015) derived T cells *in vitro*. CXCL8, a chemokine recruiting neutrophil granulocytes, was highly secreted by both ICD (3743+/-1221pg/ml, n=10) and psoriasis (6249+/-1753pg/ml, n=12) derived T cells. CXCL8 secretion by ACD-derived T cells was lower (1494+/-638pg/ml, n=8; Figure 5F). Consequently, a higher number of neutrophil granulocytes was detected in ICD (12.2+/-6,72, n=15) and psoriasis (18.6+/-4.35, n=12) lesions than in ACD (1.3+/-0.53, n=7) *in situ* (Figure 5G, H).

Beyond similarities concerning the immune cell profile, ICD and psoriasis shared induction of the inducible nitric oxidase, NOS2, in lesional skin. NOS2 is a valid metabolic marker of psoriasis [3]. In contrast, NOS2 was almost absent in ACD (Figure 5I).

As a *proof-of-concept*, an influence of blocking IL-23 on ICD was investigated. One patient suffering from severe psoriasis developed a moderate ICD 14 days after application of imiquimod, with typical development of papules and a histologic correlate in spongiosis with epidermal dyskeratoses and a

404 perivascular immune infiltration (Figure 5J). Subsequently, a psoriasis treatment with ustekinumab, an
405 IL-12p40 antibody that neutralizes effects of IL-23, was initiated. 6 weeks after initiation, imiquimod
406 was again applied to the patient in an identical setting. This time, the ICD reaction in this one patient
407 was less remarkable clinically; histopathology described a perivascular immune infiltration and an
408 unaltered epidermis (Figure 5J).

Discussion

A standardized human model of psoriasis is missing. In this study, we evaluated a commonly used mouse model of psoriasis for its possible value in the human setting. Epicutaneous application of imiquimod stimulated pDC via TLR7/8 ligation *in vivo* to induce an acute cutaneous inflammation mimicking contact dermatitis and pseudo-lymphoma. Despite clinical and histological phenotype, the human imiquimod model allows insights into the pathogenesis of psoriasis.

The principle to patch small molecules or antigens epicutaneously as a model for inflammatory skin diseases is established in atopic eczema (AE), the most common non-communicable inflammatory skin disease besides psoriasis. Here, the so-called "atopy patch test" (APT) is a recognized model of early lesions [20, 21]. Despite its limitations, the hypothesis of an immune evolution in AE from a pure T helper 2 response to a mixed immune inflitration (previously called "molecular switch") was developed from studies using the APT [22]. Thus, a standardized human patch test model is of worth to investigate the pathogenesis of a complex disease *in vivo*, even if not all aspects of the disease are covered.

Application of imiquimod over a period of 28 days induced the clinical picture of an acute contact dermatitis, over time erosions developed. After imiquimod withdrawal, the lesions were self-limited without showing clinical signs of psoriasis. In line with the clinical course, histological analysis revealed dyskeratosis, spongiosis and destruction of the epidermis with serum crusts containing neutrophil granulocytes. Severe reactions were accompanied by deep dermal lymphocytic infiltrates. Early lesions were similar to those reported in a case series that investigated cutaneous inflammation after tape stripping and short-term application of imiquimod [12].

The reaction to imiquimod showed inter-individual differences regarding kinetics and quantity, but it was monomorphic and independent of the disease background. Thus, it seems unlikely psoriasis patients are generally prone to develop psoriasis upon stimulation with imiquimod as observed in single cases [17, 23]. Furthermore, albeit the formulation of Aldara® cream is pro-inflammatory beyond TLR7/8 [24], the reaction observed in our study was dependent on imiquimod, as a vehicle control did not induce inflammation.

436 In line with the clinical and histological phenotype, we demonstrate that the transcriptome of
437 imiquimod-induced inflammation largely resembles allergic contact dermatitis (ACD) rather than
438 psoriasis. This includes major pathogenic hallmarks of ACD such as IFN-α signalling, upregulation of
439 cytotoxic granules, and apoptosis [25, 26].

440 Increasing evidence suggests that ACD is initiated by the innate immune system sensing danger [27].
441 Common antigens eliciting ACD mimic infection by stimulating pattern recognition receptors (PRRs)
442 such as TLRs [28, 29]. Also in psoriasis, PRRs and sensing danger seem to be pivotal for early
443 pathogenesis. Antimicrobial peptides, chemokines, and complexes of self-DNA or microbial DNA
444 orchestrate the stimulation of pDC to secrete IFN-α and a subsequent Th17 immune response [2, 30, 31].
445 Our study confirms that the number of TLR7+ pDCs increases upon stimulation with imiquimod. pDC
446 respond with stress signals and production of pro-inflammatory cytokines that ultimately lead to both
447 cell growth arrest [19] and a Th17 immune response. Of note, also inducible nitric oxidase (NOS2) is
448 upregulated in the course of the imiquimod-induced inflammation. NOS2 is a specific marker for
449 psoriasis that is typically not expressed in all subtypes of eczema, including ACD [3, 32].

450 Taken together, our study supports the concept that imiquimod induces an acute contact dermatitis
451 response with the special trait that pDCs act as primary sensors – and this trait is shared with human
452 psoriasis.

453 A second important difference of classical contact dermatitis reactions and imiquimod-induced
454 inflammation is the major role of IL-23. In several genetically modified mouse models, diminished
455 inflammatory responses to imiquimod could be restored by injection of IL-23, among them IL-17
456 knockout [33], ablation of nociceptive sensory neurons [34], and knockout of distinct subsets of dendritic
457 cells [15, 16]. Our study demonstrates that IL-23 is also a key driver of human imiquimod-induced
458 inflammation. This is supported by a proof-of-concept experiment of one psoriasis patient who
459 showed a diminished response to imiquimod under therapy with ustekinumab, an antibody blocking
460 IL-12p40 that is approved to treat moderate-to-severe psoriasis [35]. Of note, biologic therapies
461 inhibiting selectively IL-23 show overwhelming efficacy in treating psoriasis in clinical trials [36, 37].

In summary, triggering TLR7/8 elicits a self-limited contact dermatitis reaction mediated by pDC and IL-23 in humans. There is a discrepancy between clinical and histological phenotype on the one hand, and the molecular signature and invading immune cells on the other hand in this model. Despite these limitations, the human imiquimod patch test model might be used to investigate early pathogenic events in psoriasis.

Acknowledgements

The authors thank Jana Sänger for excellent technical support. This study was performed with samples of the biobank Biederstein of the Technical University of Munich.

References

1. Lebwohl MG, Kavanaugh A, Armstrong AW, Van Voorhees AS. US Perspectives in the Management of Psoriasis and Psoriatic Arthritis: Patient and Physician Results from the Population-Based Multinational Assessment of Psoriasis and Psoriatic Arthritis (MAPP) Survey. Am J Clin Dermatol 2016; 17:87-97.
2. Boehncke WH, Schon MP. Psoriasis. Lancet 2015; 386:983-94.
3. Quaranta M, Knapp B, Garzorz N, Mattii M, Pullabhatla V, Pennino D, et al. Intra-individual genome expression analysis reveals a specific molecular signature of psoriasis and eczema. Sci Transl Med 2014.
4. Suarez-Farinas M, Li K, Fuentes-Duculan J, Hayden K, Brodmerkel C, Krueger JG. Expanding the psoriasis disease profile: interrogation of the skin and serum of patients with moderate-to-severe psoriasis. J Invest Dermatol 2012; 132:2552-64.
5. Swindell WR, Xing X, Stuart PE, Chen CS, Aphale A, Nair RP, et al. Heterogeneity of inflammatory and cytokine networks in chronic plaque psoriasis. PLoS One 2012; 7:e34594.
6. Swindell WR, Sarkar MK, Liang Y, Xing X, Gudjonsson JE. Cross-Disease Transcriptomics: Unique IL-17A Signaling in Psoriasis Lesions and an Autoimmune PBMC Signature. J Invest Dermatol 2016; 136:1820-30.
7. Tian S, Krueger JG, Li K, Jabbari A, Brodmerkel C, Lowes MA, et al. Meta-analysis derived (MAD) transcriptome of psoriasis defines the "core" pathogenesis of disease. PLoS One 2012; 7:e44274.
8. Swindell WR, Johnston A, Carbajal S, Han G, Wohn C, Lu J, et al. Genome-wide expression profiling of five mouse models identifies similarities and differences with human psoriasis. PLoS One 2011; 6:e18266.
9. Di Domizio J, Conrad C, Gilliet M. Xenotransplantation Model of Psoriasis. Methods Mol Biol 2017; 1559:83-90.
10. Hawkes JE, Gudjonsson JE, Ward NL. The Snowballing Literature on Imiquimod-Induced Skin Inflammation in Mice: A Critical Appraisal. J Invest Dermatol 2016.
11. van der Fits L, Mourits S, Voerman JS, Kant M, Boon L, Laman JD, et al. Imiquimod-induced psoriasis-like skin inflammation in mice is mediated via the IL-23/IL-17 axis. J Immunol 2009; 182:5836-45.
12. Vinter H, Iversen L, Steiniche T, Kragballe K, Johansen C. Aldara(R)-induced skin inflammation: studies of patients with psoriasis. Br J Dermatol 2015; 172:345-53.
13. Grine L, Dejager L, Libert C, Vandenbroucke RE. Dual Inhibition of TNFR1 and IFNAR1 in Imiquimod-Induced Psoriasiform Skin Inflammation in Mice. J Immunol 2015; 194:5094-102.
14. Dickson MC, Ludbrook VJ, Perry HC, Wilson PA, Garthside SJ, Binks MH. A model of skin inflammation in humans leads to a rapid and reproducible increase in the interferon response signature: a potential translational model for drug development. Inflamm Res 2015; 64:171-83.
15. Singh TP, Zhang HH, Borek I, Wolf P, Hedrick MN, Singh SP, et al. Monocyte-derived inflammatory Langerhans cells and dermal dendritic cells mediate psoriasis-like inflammation. Nat Commun 2016; 7:13581.
16. Yoshiki R, Kabashima K, Honda T, Nakamizo S, Sawada Y, Sugita K, et al. IL-23 from Langerhans cells is required for the development of imiquimod-induced psoriasis-like

515 dermatitis by induction of IL-17A-producing gammadelta T cells. J Invest Dermatol 2014;
516 134:1912-21.
517 17. Gilliet M, Conrad C, Geiges M, Cozzio A, Thurlimann W, Burg G, et al. Psoriasis triggered by
518 toll-like receptor 7 agonist imiquimod in the presence of dermal plasmacytoid dendritic cell
519 precursors. Arch Dermatol 2004; 140:1490-5.
520 18. Lin Z, Yang C, Zhu Y, Duchi J, Fu Y, Wang Y, et al. Simultaneous dimension reduction and
521 adjustment for confounding variation. Proc Natl Acad Sci U S A 2016; 113:14662-7.
522 19. Gross CJ, Mishra R, Schneider KS, Medard G, Wettmarshausen J, Dittlein DC, et al. K+ Efflux-
523 Independent NLRP3 Inflammasome Activation by Small Molecules Targeting Mitochondria.
524 Immunity 2016; 45:761-73.
525 20. Darsow U, Laifaoui J, Kerschenlohr K, Wollenberg A, Przybilla B, Wuthrich B, et al. The
526 prevalence of positive reactions in the atopy patch test with aeroallergens and food allergens
527 in subjects with atopic eczema: a European multicenter study. Allergy 2004; 59:1318-25.
528 21. Eyerich S, Onken AT, Weidinger S, Franke A, Nasorri F, Pennino D, et al. Mutual antagonism
529 of T cells causing psoriasis and atopic eczema. N Engl J Med 2011; 365:231-8.
530 22. Eyerich K, Eyerich S, Biedermann T. The Multi-Modal Immune Pathogenesis of Atopic
531 Eczema. Trends Immunol 2015; 36:788-801.
532 23. Patel U, Mark NM, Machler BC, Levine VJ. Imiquimod 5% cream induced psoriasis: a case
533 report, summary of the literature and mechanism. Br J Dermatol 2011; 164:670-2.
534 24. Walter A, Schafer M, Cecconi V, Matter C, Urosevic-Maiwald M, Belloni B, et al. Aldara
535 activates TLR7-independent immune defence. Nat Commun 2013; 4:1560.
536 25. Eyerich K, Bockelmann R, Pommer AJ, Foerster S, Hofmeister H, Huss-Marp J, et al.
537 Comparative in situ topoproteome analysis reveals differences in patch test-induced eczema:
538 cytotoxicity-dominated nickel versus pleiotrope pollen reaction. Exp Dermatol 2010; 19:511-
539 7.
540 26. Traidl C, Sebastiani S, Albanesi C, Merk HF, Puddu P, Girolomoni G, et al. Disparate cytotoxic
541 activity of nickel-specific CD8+ and CD4+ T cell subsets against keratinocytes. J Immunol
542 2000; 165:3058-64.
543 27. Martin SF. Allergic contact dermatitis: xenoinflammation of the skin. Curr Opin Immunol
544 2012; 24:720-9.
545 28. Kaplan DH, Igyarto BZ, Gaspari AA. Early immune events in the induction of allergic contact
546 dermatitis. Nat Rev Immunol 2012; 12:114-24.
547 29. Schmidt M, Raghavan B, Muller V, Vogl T, Fejer G, Tchaptchet S, et al. Crucial role for human
548 Toll-like receptor 4 in the development of contact allergy to nickel. Nat Immunol 2010;
549 11:814-9.
550 30. Lande R, Gregorio J, Facchinetti V, Chatterjee B, Wang YH, Homey B, et al. Plasmacytoid
551 dendritic cells sense self-DNA coupled with antimicrobial peptide. Nature 2007; 449:564-9.
552 31. Dombrowski Y, Peric M, Koglin S, Kammerbauer C, Goss C, Anz D, et al. Cytosolic DNA triggers
553 inflammasome activation in keratinocytes in psoriatic lesions. Sci Transl Med 2011; 3:82ra38.
554 32. Garzorz N, Krause L, Lauffer F, Atenhan A, Thomas J, Stark SP, et al. A novel molecular disease
555 classifier for psoriasis and eczema. Exp Dermatol 2016.
556 33. El Malki K, Karbach SH, Huppert J, Zayoud M, Reissig S, Schuler R, et al. An alternative
557 pathway of imiquimod-induced psoriasis-like skin inflammation in the absence of interleukin-
558 17 receptor a signaling. J Invest Dermatol 2013; 133:441-51.
559 34. Riol-Blanco L, Ordovas-Montanes J, Perro M, Naval E, Thiriot A, Alvarez D, et al. Nociceptive
560 sensory neurons drive interleukin-23-mediated psoriasiform skin inflammation. Nature 2014;
561 510:157-61.
562 35. Griffiths CE, Strober BE, van de Kerkhof P, Ho V, Fidelus-Gort R, Yeilding N, et al. Comparison
563 of ustekinumab and etanercept for moderate-to-severe psoriasis. N Engl J Med 2010;
564 362:118-28.
565 36. Gordon KB, Duffin KC, Bissonnette R, Prinz JC, Wasfi Y, Li S, et al. A Phase 2 Trial of
566 Guselkumab versus Adalimumab for Plaque Psoriasis. N Engl J Med 2015; 373:136-44.
567 37. Puig L. The role of IL 23 in the treatment of psoriasis. Expert Rev Clin Immunol 2017.

Figure legends

Fig. 1 Topical application of imiquimod induces a self-limited acute contact dermatitis reaction. **A** Representative clinical course of the reaction to imiquimod (ICD) in one patient with strong reactivity and study design. Imiquimod was applied occlusive twice weekly (scheme) until day 28, punch biopsy specimens were obtained at day 4, 14, and 28. **B** H&E stainings of ICD lesions over time. Bars indicate 100µm. **C** Similarity of non-involved skin (pre-IMQ) and ICD lesions to psoriasis and eczema, respectively, as assessed in histology scores. ICD: Imiquimod induced contact dermatitis *p<0.05; **p<0.01; ***p<0.001; ****p<0.0001.

Fig. 2 The ICD transcriptome closely overlaps with ACD and to a lesser extend with psoriasis. **A** acPCA visualization of whole genome expression analysis including 95% confidence intervals per group of ICD (n=16), ACD (n=10), and psoriasis (n=24) as compared to non-involved skin. **B** Correlation of fold induction of all genes of ICD and ACD or of ICD and psoriasis, respectively. gray: genes significantly regulated in both lesions, green and red: genes significantly regulated in ACD and psoriasis, respectively; blue: genes significantly regulated in ICD. black: not significantly regulated genes. **C** Overlap of significantly regulated genes as shown in Venn Plots. Percentages indicate the relative number of genes significantly regulated in either ACD or psoriasis, respectively, that are also regulated significantly in ICD. Smaller Venn Plots indicate the overlap of top hit genes with a log2 fold induction >2.5.

Fig. 3 Both ICD and ACD reactions are dominated by immune-mediated cytotoxicity. **A** Comparative transcriptome analysis of lesional ICD (n=16), ACD (n=10), and psoriasis (n=24) revealed pathways related to apoptosis in both ICD and ACD, but not in psoriasis; outtake of whole network as indicated at right side. blue: pathways regulated exclusively in ICD; yellow: pathways regulated in ICD and ACD. Font size indicates the relative percentage of regulated genes within the pathway (small size: 0-40% of all genes; medium size: 40-60%; big size: >60%). **B** Representative immune-histochemical stainings of lesional ICD, ACD, and psoriasis for CD4 (left column) and CD8 (right column). Bars indicate 100µm. **C** CD4/CD8 ratio for non-involved skin (pre IMQ), ICD, ACD,

and psoriasis as calculated from the mean numbers of cells/ visual field in immune-histochemical stainings. Shown is the mean +/- SEM. **D** Flow cytometric analysis of T cells isolated of ICD, ACD, or psoriasis lesions, respectively. Shown is a merge of all patients, with each colour representing one patient. Left column: surface stainings of CD4 and CD8. Middle column: combined surface staining of CD4 (middle) or CD8 (right column) and intracellular cytokine staining for IFN-γ. Numbers in each quadrant give relative percentage. **E** IFN-γ or CXCL-10 secretion into supernatant of primary T cells derived from ICD, ACD, or psoriasis lesions, respectively, 72 hours after T cell receptor stimulation. Box plots indicate median and 95% confidence intervals. **F** Representative immune-histochemical stainings for caspase-3 in one ICD, ACD, or psoriasis lesion, respectively, and quantitative numbers of Caspase 3 positive cells /visual field. Bars indicate 100µm. *$p<0.05$; **$p<0.01$; ***$p<0.001$.

Fig. 4 pDC are the primary sensory cells in ICD. **A** Comparative transcriptome analysis of lesional ICD (n=16), ACD (n=10), and psoriasis (n=24) revealed unique pathways for ICD (blue) in the type 1 IFN-signalling cascade; outtake of whole network shown in frame and in Figure S3. **B** The number of BDCA-2+ cells and staining intensity of TLR7 increased during the course of the reaction, as illustrated in one representative patient at day 0 (left) and day 14 (middle). **C** The number of BDCA-2+ cells ($r^2=0.610$) and staining intensity for TLR7 ($r^2=0.505$) *in situ* correlated with the clinical severity of the reaction. **D** Oxygen consumption rate (OCR, left graph) and extracellular acidification (ECAR) of primary human pDC stimulated with imiquimod (IMQ), R848 or gardiquimod (GAR) over time as compared to unstimulated pDC. Arrows indicate addition of compound or Rotenone application. **E** Real-time PCR analysis of primary human pDC stimulated with imiquimod (IMQ), R848, or gardiquimod (GAR) for 6 hours. Shown is the fold induction as compared to unstimulated pDC.

Fig. 5 ICD is a Th17-deviated contact dermatitis. **A** Comparative transcriptome analysis of lesional ICD (n=16), ACD (n=10), and psoriasis (n=24) revealed the IL-23 pathway is shared by ICD and psoriasis (dark grey); outtake of whole network as indicated at right side. Font size indicates the relative percentage of regulated genes within the pathway (smaller size: 40-60%; big size: >60%). **B** Genes of the IL-23 pathway significantly regulated in ICD, psoriasis, and/or ACD. **C** Representative

immune-histochemical stainings of ICD, ACD, and psoriasis for IL-17. **D** Quantitative analysis of IL-17+ cells in immune-histochemical stainings. Shown is the mean +/- SEM, each symbol represents one sample. **E** Flow cytometric analysis of T cells isolated of ICD, ACD, or psoriasis lesions, respectively. Shown is a merge of all patients, with each colour representing one patient. Intracellular cytokine staining for IL-17 (x-axis) and IL-22 (y-axis). Numbers in each quadrant give relative percentage. **F** IL-17, CXCL-8, or IL-6 secretion into supernatant of primary T cells derived from ICD, ACD, or psoriasis lesions, respectively, 72 hours after T cell receptor stimulation. Box plots indicate median and 95% confidence intervals. **G** Representative immune-histochemical stainings of ICD, ACD, and psoriasis for neutrophil elastase (NET). **H** Quantitative analysis of NET+ cells in immune-histochemical stainings. Shown is the mean +/- SEM, each symbol represents one sample. **I** Immune-fluorescence stainings of one representative ICD, ACD, and psoriasis lesion. **J** Clinical and histological reaction after 9 days of imiquimod application in one psoriasis patient prior to and 6 weeks under ustekinumab therapy.

Fig. 1

A

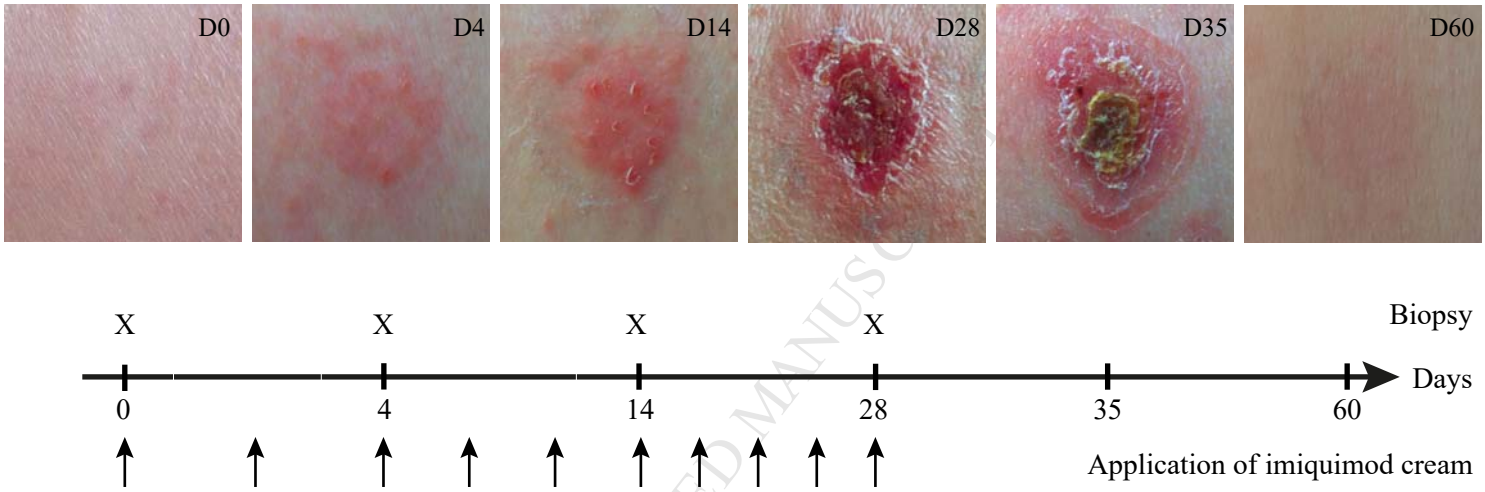

B

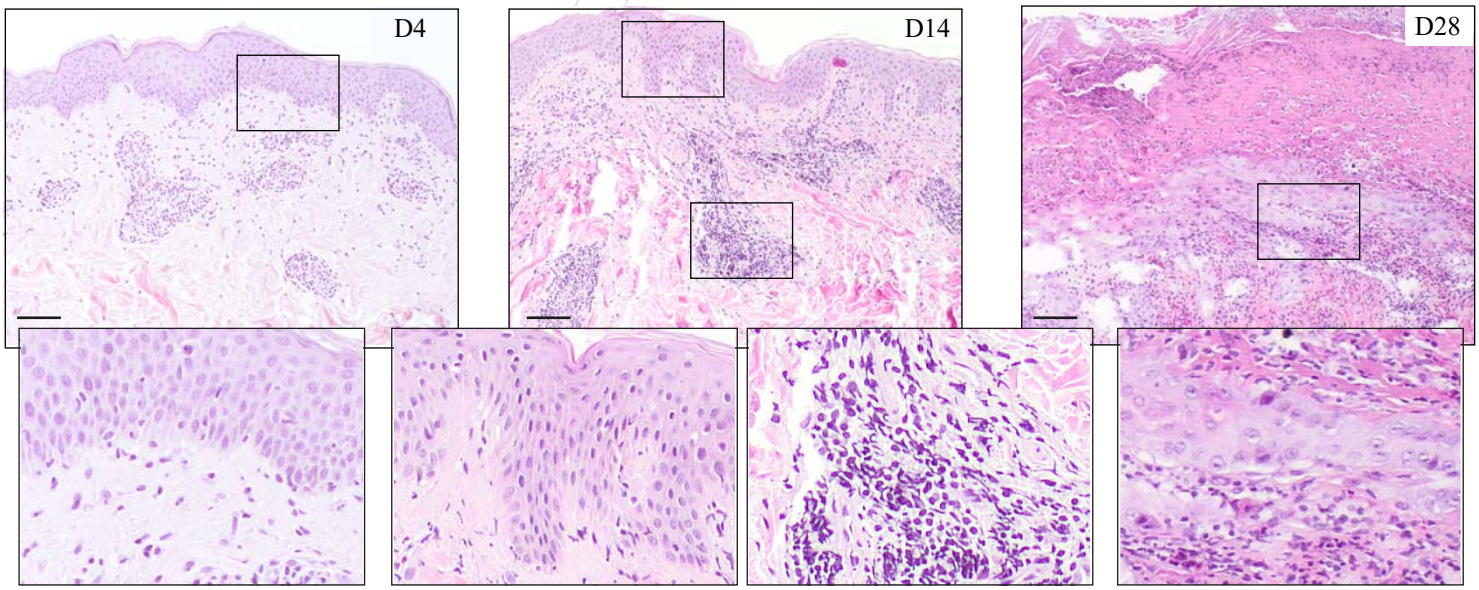

C

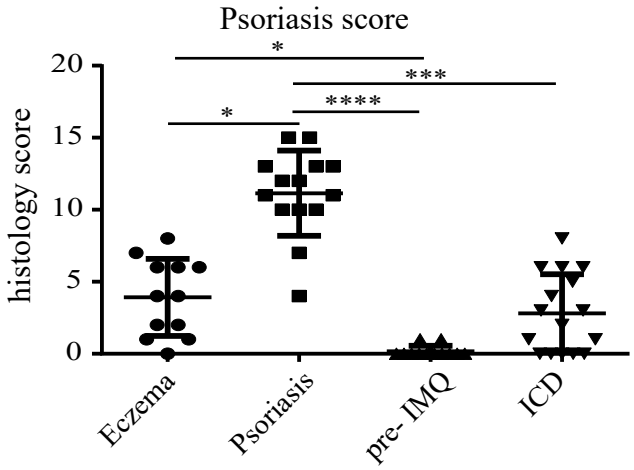

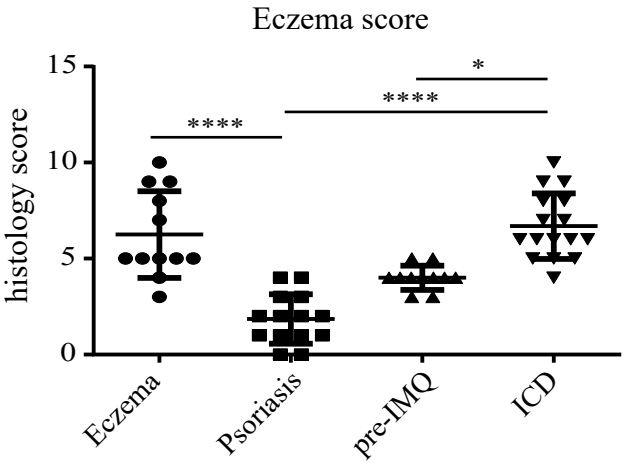

Fig. 2

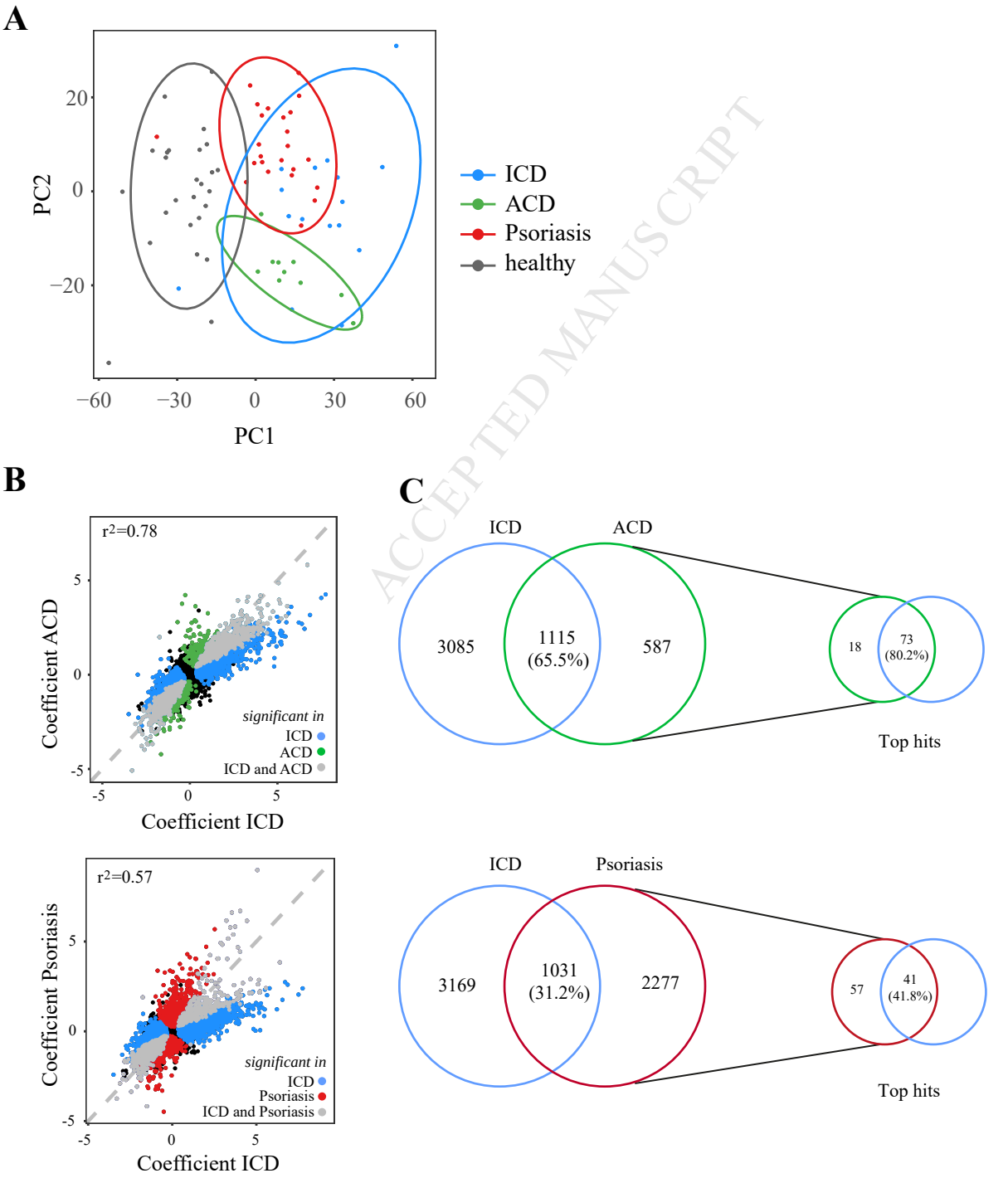

Fig. 3

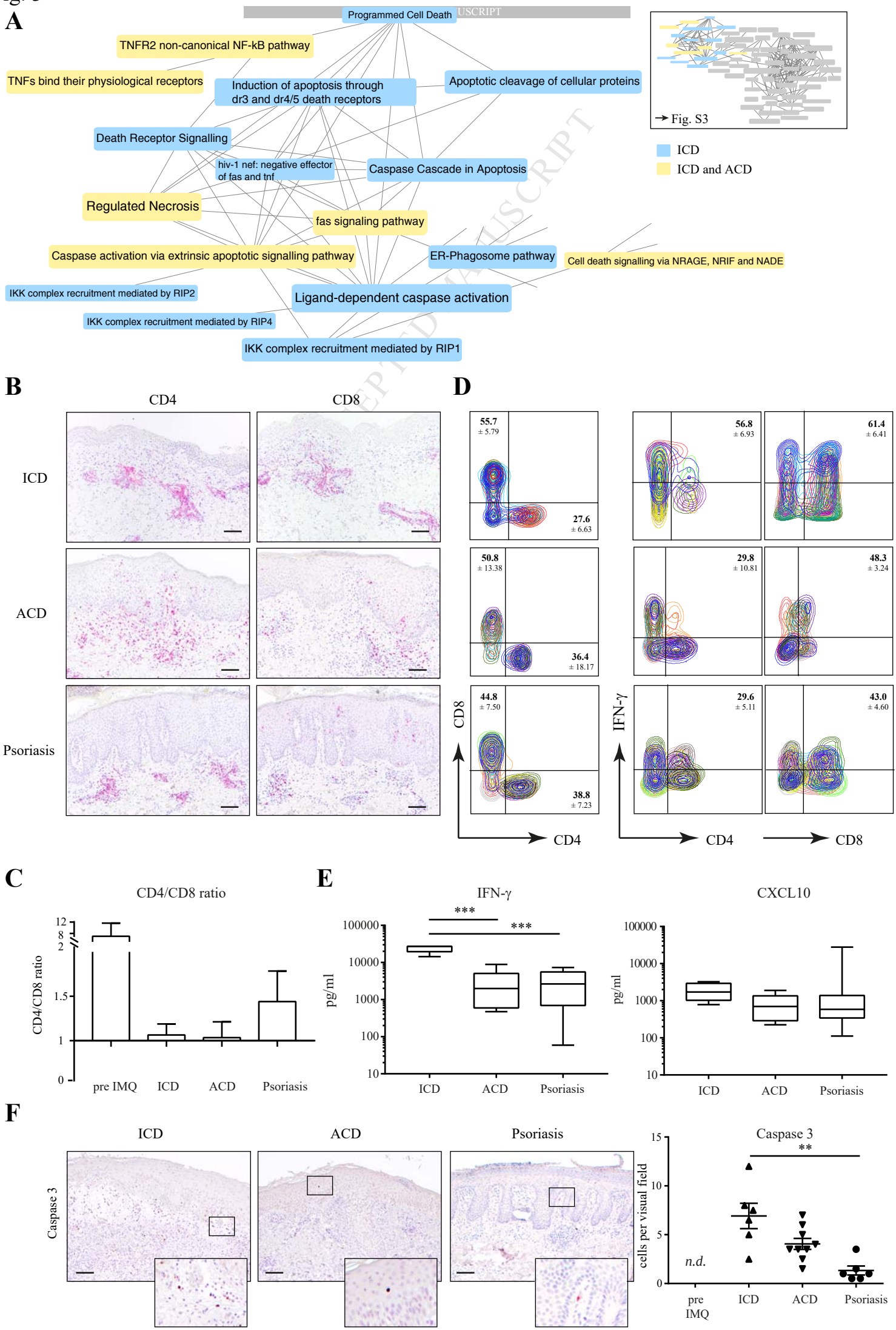
A
Programmed Cell Death
TNFR2 non-canonical NF-kB pathway
TNFs bind their physiological receptors
Induction of apoptosis through dr3 and dr4/5 death receptors
Apoptotic cleavage of cellular proteins
Death Receptor Signalling
hiv-1 nef: negative effector of fas and tnf
Caspase Cascade in Apoptosis
Regulated Necrosis
fas signaling pathway
Caspase activation via extrinsic apoptotic signalling pathway
ER-Phagosome pathway
Cell death signalling via NRAGE, NRIF and NADE
IKK complex recruitment mediated by RIP2
Ligand-dependent caspase activation
IKK complex recruitment mediated by RIP4
IKK complex recruitment mediated by RIP1
→ Fig. S3
ICD
ICD and ACD
B
CD4
CD8
ICD
ACD
Psoriasis
D
55.7 ± 5.79
27.6 ± 6.63
56.8 ± 6.93
61.4 ± 6.41
50.8 ± 13.38
36.4 ± 18.17
29.8 ± 10.81
48.3 ± 3.24
44.8 ± 7.50
38.8 ± 7.23
29.6 ± 5.11
43.0 ± 4.60
CD8
IFN-γ
CD4
CD4
CD8
C
CD4/CD8 ratio
CD4/CD8 ratio
pre IMQ
ICD
ACD
Psoriasis
E
IFN-γ
CXCL10
***
***
pg/ml
ICD
ACD
Psoriasis
F
ICD
ACD
Psoriasis
Caspase 3
Caspase 3
**
cells per visual field
n.d.
pre IMQ
ICD
ACD
Psoriasis

Fig. 4

A

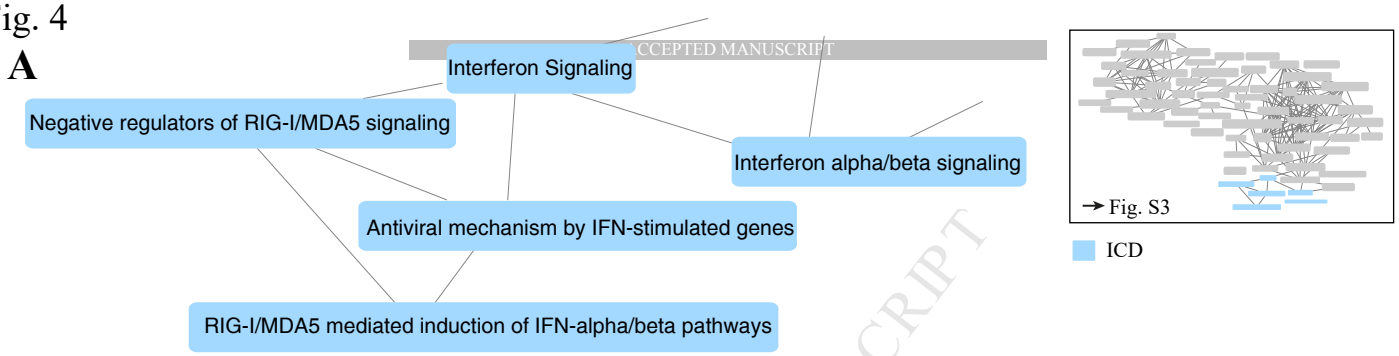

B

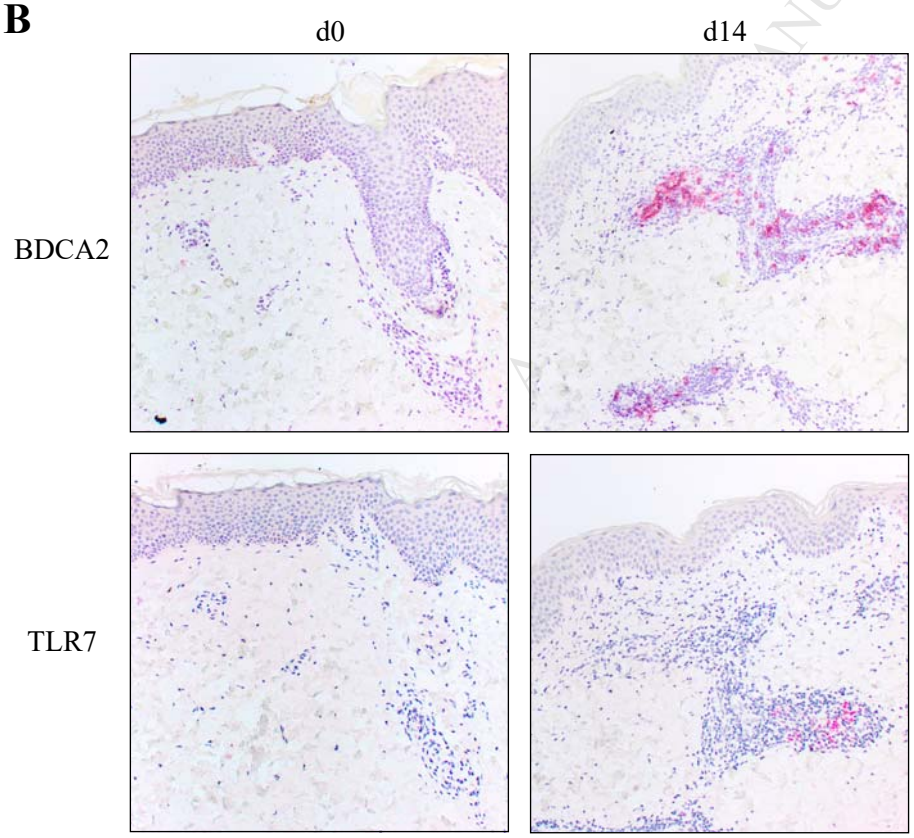

C

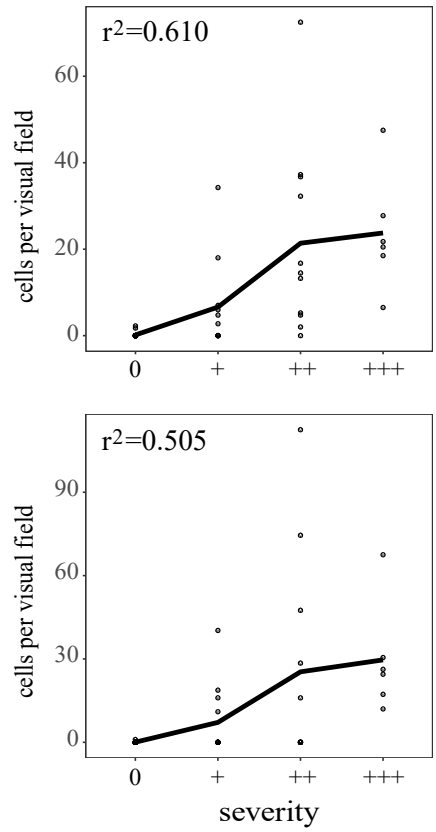

D

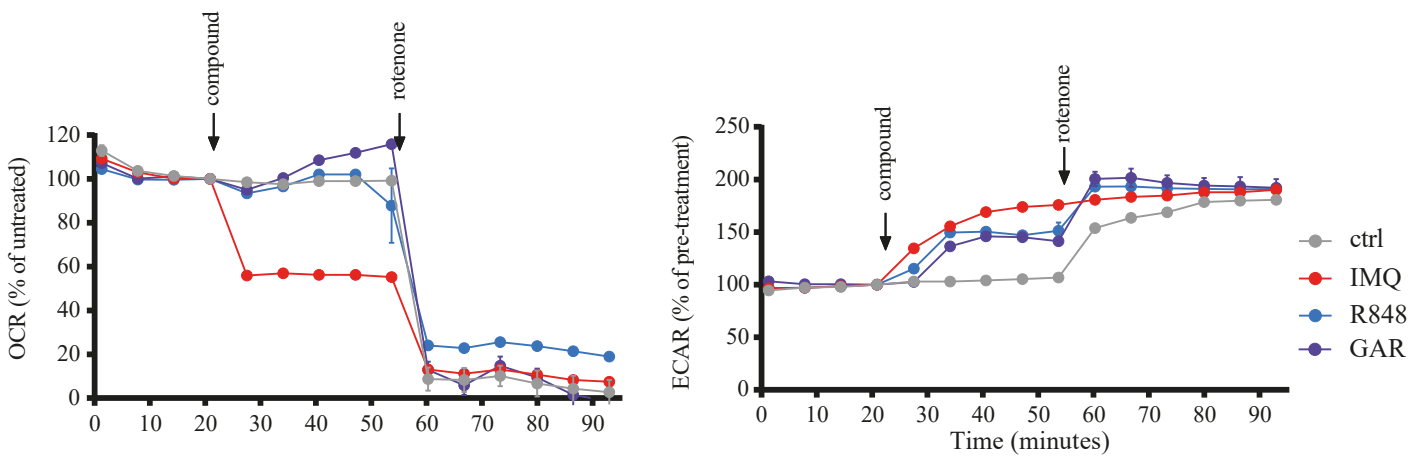

E

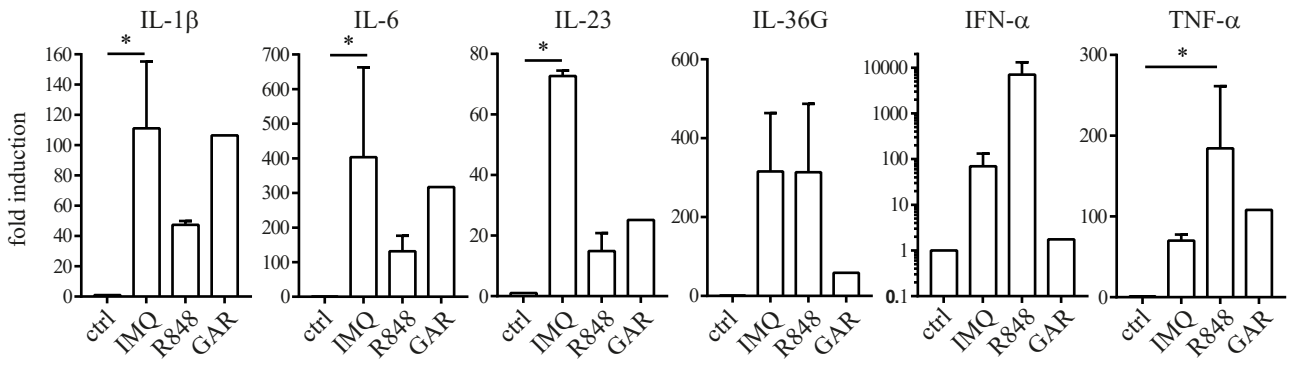

Fig. 5

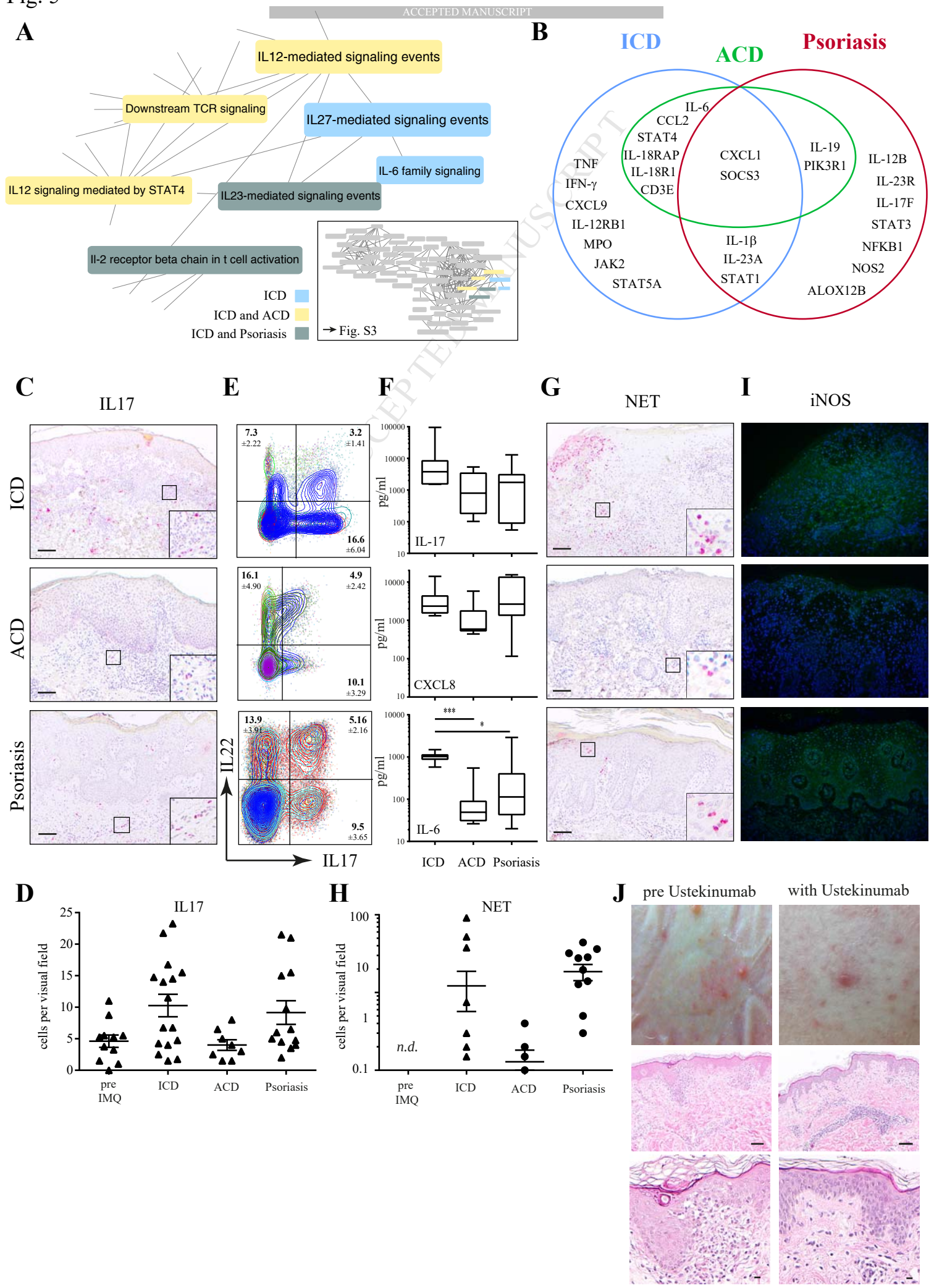

Table 1. Patient characteristics

ID of volunteer	Sex	Age	Background	D4	D14	D28
1	m	35	Atopic eczema	+	++	+++
2	f	61	Healthy	++	+	+
3	f	42	Psoriasis	+++	++	+
4	f	29	Healthy	+	++	+++
5	f	45	Atopic eczema	+	+++	++
6	m	33	Psoriasis	+	+++	++/+++
7	m	46	Healthy	0		
8	f	40	Psoriasis and atopic eczema	+	+	++
9	f	51	Psoriasis	++	+++	+
10	f	53	Healthy	++	+	+
11	f	59	Psoriasis	0		
12	f	70	Atopic eczema	0		
13	f	47	Healthy	+/++	+	++
14	f	55	Healthy	+	++	+
15	m		Psoriasis	0	0	n.d.
16	m		Psoriasis	+	++	n.d.
17	f		Psoriasis	+	+	n.d.
18	m	23	Psoriasis and atopic eczema	++	++	n.d.

Supplementary files

TLR7/8 agonists stimulate plasmacytoid dendritic cells to initiate a Th17-deviated acute contact dermatitis in humans

Natalie Garzorz-Stark[1,†,*], Felix Lauffer[†,1], Linda Krause[2], Jenny Thomas[3], Anne Atenhan[3], Regina Franz[1], Sophie Roenneberg[1], Alexander Boehner[1], Manja Jargosch[3], Richa Batra[2], Nikola S. Mueller[2], Stefan Haak[3], Christina Groß[4], Olaf Groß[4], Claudia Traidl-Hoffmann[5], Fabian J. Theis [2,6], Carsten B Schmidt-Weber[3], Tilo Biedermann[1], Stefanie Eyerich[3, ††], Kilian Eyerich[1, ††]

Affiliations:

[1] Department of Dermatology and Allergy, Technical University of Munich, Munich, Germany

[2] Institute of Computational Biology, Helmholtz Center Munich, Neuherberg, Germany, Member of the German Center for Lung Research (DZL)

[3] ZAUM – Center of Allergy and Environment, Technical University and Helmholtz Center Munich, Munich, Germany, Member of the German Center for Lung Research (DZL)

[4] Institute for Clinical Chemistry and Pathobiochemistry, Technical University of Munich, Munich, Germany

[5] Chair and Institute of Environmental Medicine UNIKAT, Technical University and Helmholtz Center Munich, Augsburg, Germany

[6] Department of Mathematics, Technical University of Munich, Garching, Germany

*To whom correspondence should be addressed: natalie.garzorz@tum.de

[†] N.G. and F.L. contributed equally to this work

[†] S.E. and K.E. contributed equally to this work

Supplementary methods

Statistical analysis

For visual comparison of genes in respective pathways, absolute foldchanges were plotted next to each other. Quantification was done by calculating Pearson's product-moment correlation coefficient between the fold changes of all genes in the pathways and its 95% confidence interval.

Isolation of mouse pDC

Immune cells from murine spleen and thymus were isolated by mechanical disruption of the organ and single cell suspension was obtained by passing the cell solution through a nylon cell strainer. Bone marrow cells were isolated by flushing tibias and femurs with PBS. Cells of all organs were pooled and erythrocytes lysed. For isolation of pDC the Murine Plasmacytoid Dendritic Cell kit (Miltenyi Biotech) was used.

Double staining immunehistochemestry

Tissue samples were fixed in 10% formalin solution and embedded in paraffin. 4µm sections were cut. After deparaffinization and rehydration, epitope retreaval in boiling EDTA buffer (pH 8) was performed. Sections were incubated with the primary antibodies (rabbit anti-TLR7 (Abcam), mouse anti-CD303 (Dendritics) antibody) over night at 4 °C. ZytoChem-Plus Double Stain Polymer-Kit, Permanent AP red Kit and Permanent HRP green Kit (Zytomed Systems) were used to visualize TLR7 (anti-rabbit AP polymer and AP red chromogene) and CD303 (anti-mouse HRP polymer and HRP green chromogen) bound primary antibodies.

Supplementary figure legends

Tbl. S1 Pathways regulated in ICD, ACD, and psoriasis, respectively.

Fig. S1 Application of Aldara® vehicle not containing imiquimod does not induce ICD. Shown is a patient where Aldara® and Aldara® vehicle were patched occlusively over a period of 28 days twice weekly.

Fig. S2 The ICD transcriptome does not correlate closely to atopic eczema. **A** Correlation of all genes of ACD and eczema. grey: genes significantly regulated in both lesions; green: genes regulated in eczema; blue: genes regulated in ACD; black: not significantly regulated genes. **B** CD4/CD8 ratio of eczema lesions (n=15)

Fig. S3 Comparative transcriptome analysis of lesional ICD (n=16), ACD (n=10), and psoriasis (n=24). blue: pathways regulated exclusively in ICD; yellow: pathways regulated in ICD and ACD. dark grey: pathways regulated in ICD and psoriasis. Font size indicates the relative percentage of regulated genes within the pathway (small size: 0-40% of all genes; medium size: 40-60%; big size: >60%).

Fig. S4 *In situ* expression of CD4+ and CD8+ T cells in ICD, ACD, and psoriasis. Quantitative analysis of CD4+ as well as CD8+ cells in immune-histochemical stainings. Shown is the mean +/- SEM, each symbol represents one sample.

Fig. S5 Differentially regulated genes within the pathway "apopotosis". **A** Shown is the absolute fold change of each gene within the pathway "apoptosis" of the Reactome database in ICD (left) and ACD (right side), with significantly upregulated genes highlighted in blue and significantly downregulated genes highlighted in yellow. **B** Correlation analysis of genes related to apoptosis. Shown are fold changes of genes in ICD lesions (x axis) versus fold changes of genes in psoriasis (y axis, red dots and line) or ACD (y axis, green dots and line), respectively. Lines indicate degree of correlation.

Fig. S6 BDCA2+TLR7+ cells in ACD and psoriasis. **A** Double immunehistochemistry labelling of BDCA2 (green) and TLR7 (red) indicates double positive pDC in ICD. Shown is one representative

staining. Bar indicates 20µm. **B** Quantitative analysis of CD4+ as well as CD8+ cells in immune-histochemical stainings. Shown is the mean +/- SEM, each symbol represents one sample.

Fig. S7 Differentially regulated genes from the pathway "interferon alpha/beta signalling". Shown is the absolute fold change of each gene within the pathway "interferon alpha/ beta signalling" of the Reactome database in comparison of ICD and psoriasis (left) and ICD and ACD (right side), with significantly upregulated genes highlighted in blue.

Fig. S8 Extracellular flux analysis of murine pDC. Oxygen consumption rate (OCR, left graph) and extracellular acidification (ECAR) of primary human pDC stimulated with imiquimod (IMQ), R848 or gardiquimod (GAR) over time as compared to unstimulated pDC. Arrows indicate addition of compound or Rotenone application.

Fig. S9 Differentially regulated genes from the IL-23 pathway. Shown is the absolute fold change of each gene within the pathway "IL-23 signalling" of the Reactome database in comparison of ICD and psoriasis (left), ICD and ACD (middle), and psoriasis and ACD (right side), with significantly upregulated genes highlighted in blue and significantly downregulated genes highlighted in yellow.

Table S1. Pathways regulated in ICD, ACD, and psoriasis, respectively.

pathway	set size	candidates contained	p-value	q-value
IL23-mediated signaling events	37(37)	18 (48.6%)	0.000111	0.00172
IL12-mediated signaling events	64(58)	36 (62.1%)	5.11e-12	4.92e-10
Antigen processing-Cross presentation	49(43)	29 (67.4%)	3.05e-11	2.45e-09
Generation of second messenger molecules	38(26)	19 (73.1%)	1.05e-08	6.31e-07
TCR signaling	69(55)	29 (52.7%)	1.04e-07	5.56e-06
PD-1 signaling	28(18)	14 (77.8%)	2.74e-07	1.32e-05
Ligand-dependent caspase activation	17(16)	13 (81.2%)	3.06e-07	1.34e-05
TCR signaling in naïve CD8+ T cells	56(50)	26 (52.0%)	6.78e-07	2.72e-05
Phosphorylation of CD3 and TCR zeta chains	27(17)	13 (76.5%)	1.06e-06	3.91e-05
TCR signaling in naïve CD4+ T cells	70(63)	29 (46.0%)	3.97e-06	0.00012
Regulated Necrosis	16(16)	12 (75.0%)	4.00E-06	0.00012
Chemokine receptors bind chemokines	50(45)	23 (51.1%)	4.38e-06	0.000124
IL27-mediated signaling events	26(26)	16 (61.5%)	5.5e-06	0.00014
CXCR4-mediated signaling events	88(80)	34 (42.5%)	5.53e-06	0.00014
Caspase Cascade in Apoptosis	57(55)	26 (47.3%)	6.8e-06	0.000164
Interferon Signaling	71(56)	26 (46.4%)	1.03e-05	0.000234
TNFR2 non-canonical NF-kB pathway	52(47)	23 (48.9%)	1.12e-05	0.000234
Caspase activation via extrinsic apoptotic signalling pathway	28(26)	15 (57.7%)	3.23e-05	0.000648
the co-stimulatory signal during t-cell activation	21(16)	11 (68.8%)	3.88e-05	0.000746
Programmed Cell Death	125(119)	43 (36.1%)	4.66e-05	0.000862
Downstream signaling in naïve CD8+ T cells	68(57)	25 (43.9%)	5.01e-05	0.000892
IL12 signaling mediated by STAT4	32(28)	15 (53.6%)	0.000103	0.00166
Costimulation by the CD28 family	75(63)	26 (41.3%)	0.000124	0.0018
ER-Phagosome pathway	24(23)	13 (56.5%)	0.000147	0.00196
Negative regulators of RIG-I/MDA5 signaling	25(23)	13 (56.5%)	0.000147	0.00196
induction of apoptosis through dr3 and dr4/5 death receptors	23(23)	13 (56.5%)	0.000147	0.00196
Endogenous TLR signaling	27(24)	13 (54.2%)	0.000261	0.0033
ras-independent pathway in nk cell-mediated cytotoxicity	22(16)	10 (62.5%)	0.000289	0.00356
Interferon alpha/beta signaling	27(19)	11 (57.9%)	0.000364	0.00418
RIG-I/MDA5 mediated induction of IFN-alpha/beta pathways	57(53)	22 (41.5%)	0.000365	0.00418
Apoptotic cleavage of cellular proteins	39(37)	17 (45.9%)	0.000406	0.00455
fas signaling pathway (cd95)	20(20)	11 (55.0%)	0.000661	0.00723
Interleukin-6 family signaling	27(26)	13 (50.0%)	0.00072	0.00753
TNFs bind their physiological receptors	30(26)	13 (50.0%)	0.00072	0.00753
Growth hormone receptor signaling	19(18)	10 (55.6%)	0.00106	0.0106
Antigen Presentation: Folding, assembly and peptide loading of class I MHC	24(21)	11 (52.4%)	0.00113	0.0111
hiv-1 nef: negative effector of fas and tnf	53(51)	20 (39.2%)	0.00156	0.015
Rho GTPase cycle	145(130)	41 (31.5%)	0.00172	0.0162
Initial triggering of complement	104(19)	10 (52.6%)	0.00182	0.0165
eicosanoid metabolism	23(22)	11 (50.0%)	0.00185	0.0165
Regulation of RAC1 activity	39(35)	15 (42.9%)	0.0021	0.0181
Death Receptor Signalling	44(42)	17 (40.5%)	0.0023	0.0194
Hedgehog signaling events mediated by Gli proteins	50(46)	18 (39.1%)	0.0027	0.022
IKK complex recruitment mediated by RIP1	26(23)	11 (47.8%)	0.0029	0.0232

Downstream TCR signaling	48(36)	15 (41.7%)	0.00294	0.0232
Class I PI3K signaling events	46(43)	17 (39.5%)	0.00309	0.024
Thromboxane A2 receptor signaling	57(51)	19 (37.3%)	0.00399	0.029
Beta2 integrin cell surface interactions	30(27)	12 (44.4%)	0.00403	0.029
Interaction between L1 and Ankyrins	30(27)	12 (44.4%)	0.00403	0.029
RAC1 signaling pathway	54(52)	19 (36.5%)	0.00511	0.0356
GPVI-mediated activation cascade	54(52)	19 (36.5%)	0.00511	0.0356
Antiviral mechanism by IFN-stimulated genes	34(28)	12 (42.9%)	0.00577	0.0391
Urokinase-type plasminogen activator (uPA) and uPAR-mediated signaling	43(42)	16 (38.1%)	0.0062	0.0414
role of mef2d in t-cell apoptosis	31(25)	11 (44.0%)	0.0064	0.0422
inactivation of gsk3 by akt causes accumulation of b-catenin in alveolar macrophages	42(39)	15 (38.5%)	0.00717	0.046
Signaling events mediated by Stem cell factor receptor (c-Kit)	52(50)	18 (36.0%)	0.00756	0.0472
t cell receptor signaling pathway	55(50)	18 (36.0%)	0.00756	0.0472
Regulation of RhoA activity	49(43)	16 (37.2%)	0.00804	0.0496
RHO GTPases Activate WASPs and WAVEs	37(36)	14 (38.9%)	0.00828	0.0504
il-2 receptor beta chain in t cell activation	48(47)	17 (36.2%)	0.00882	0.0519
L13a-mediated translational silencing of Ceruloplasmin expression	129(97)	30 (30.9%)	0.00907	0.0519
Cell death signalling via NRAGE, NRIF and NADE	78(70)	23 (32.9%)	0.0097	0.0549

Fig. S1

Aldara vehicle Aldara cream

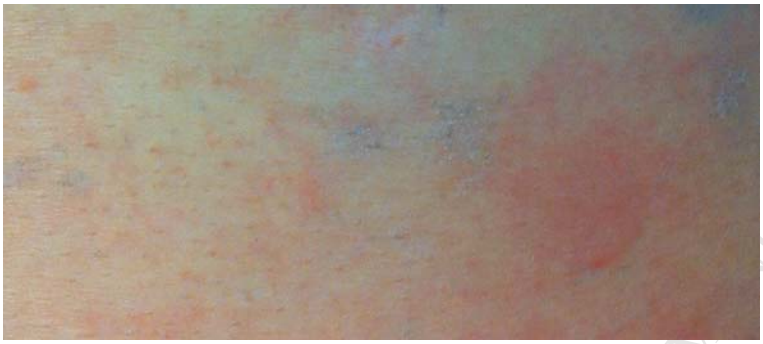

Fig. S2

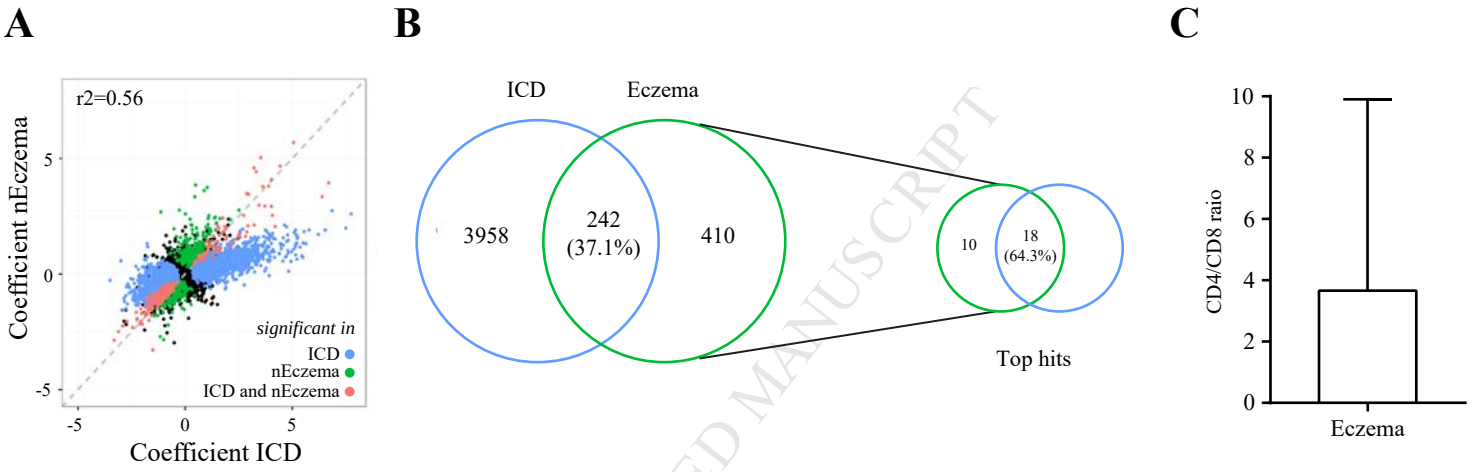

Fig. S3

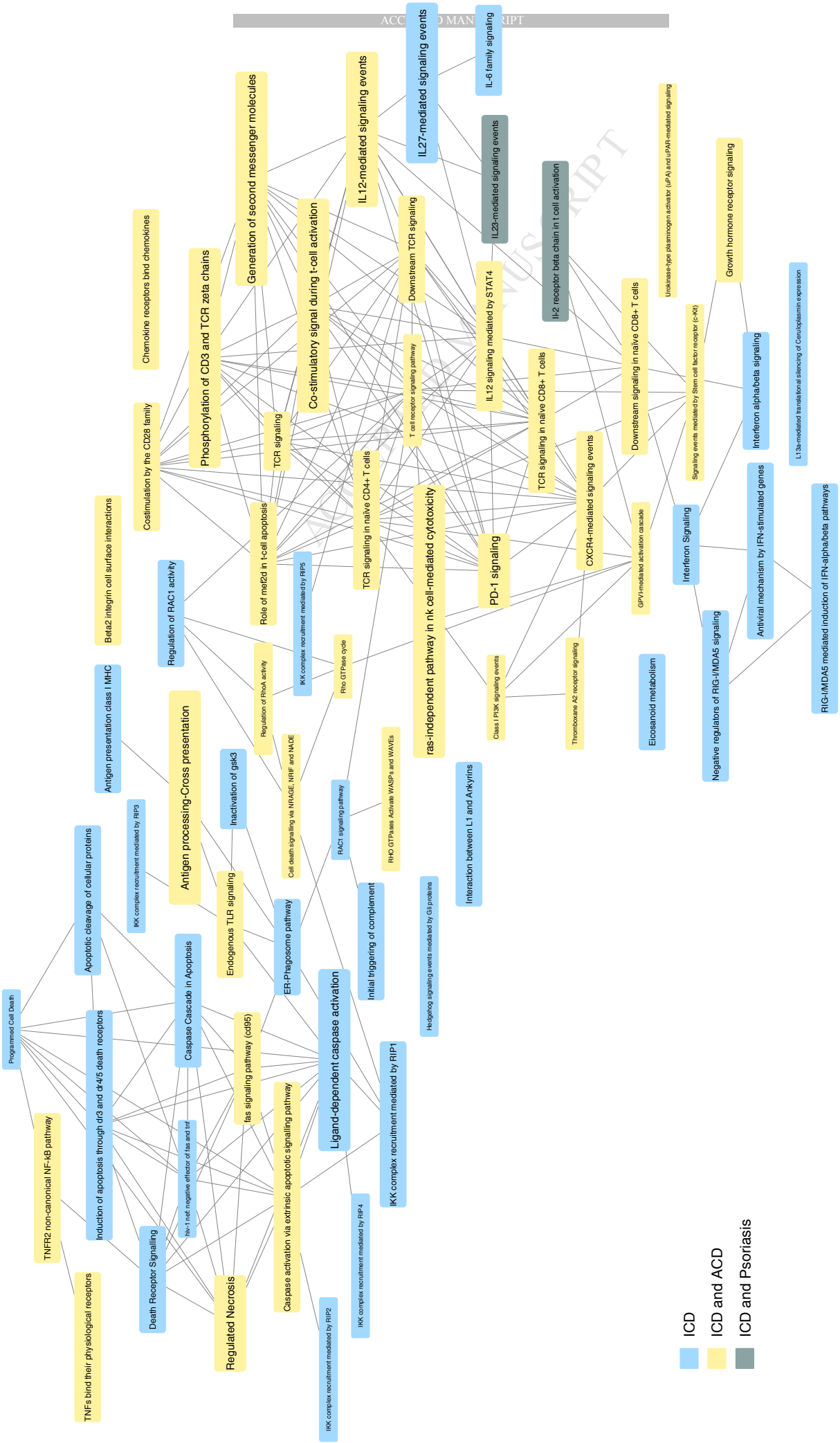

Fig. S4

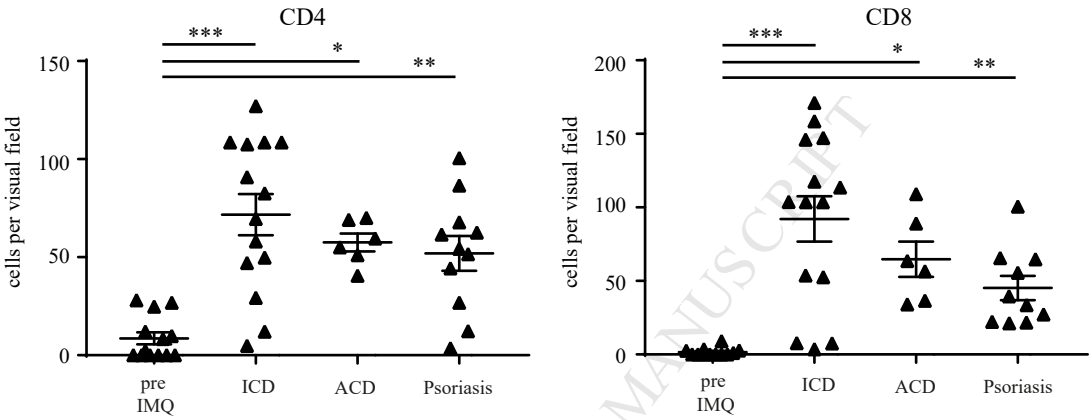

Fig. S5

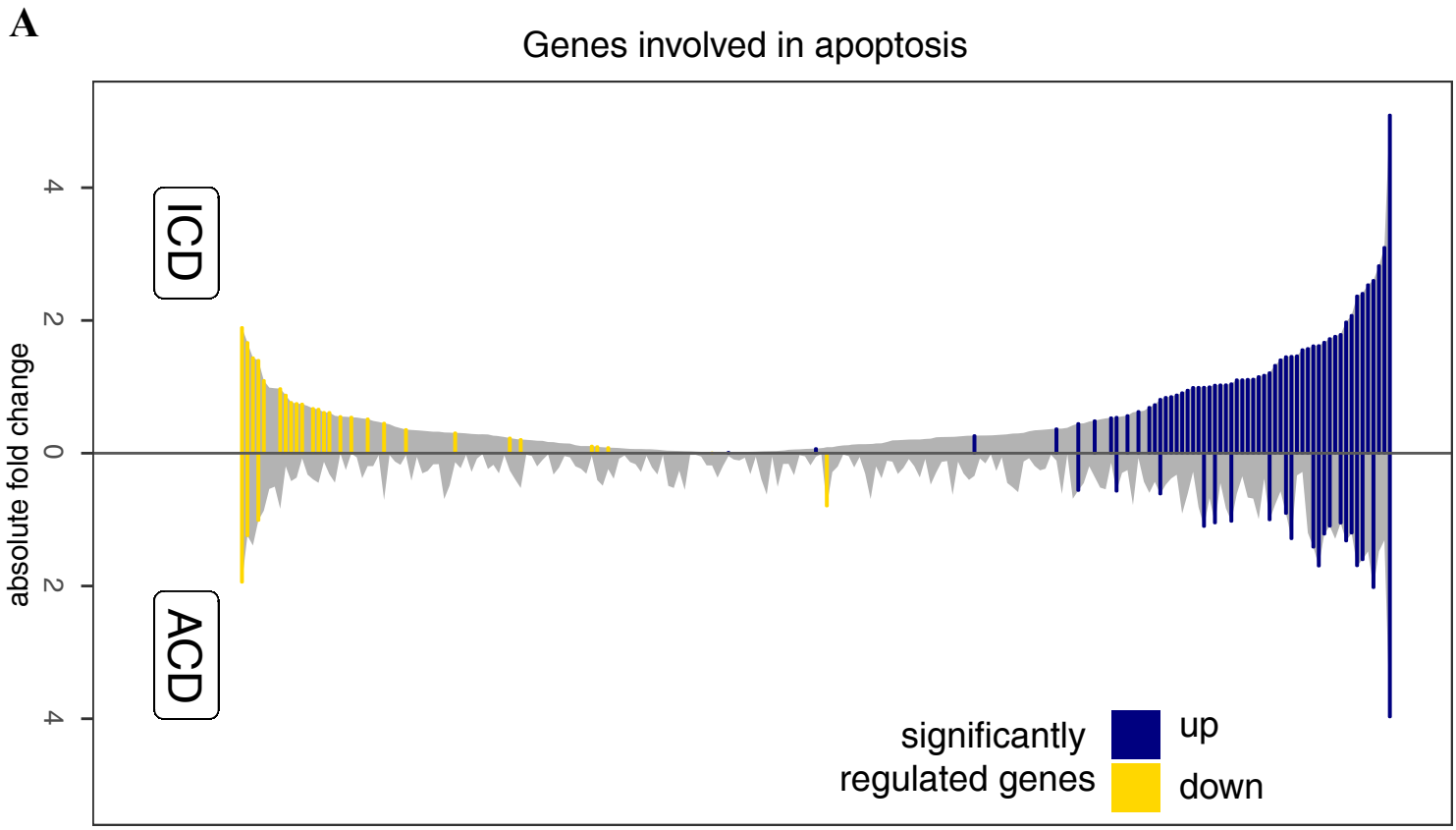

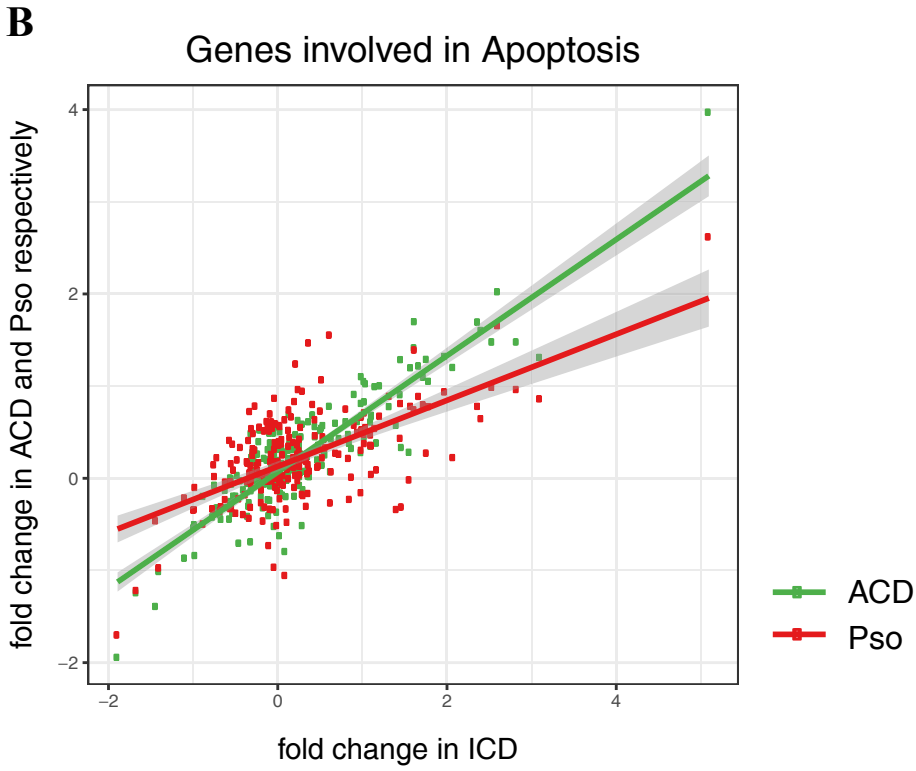

Fig. S6

A

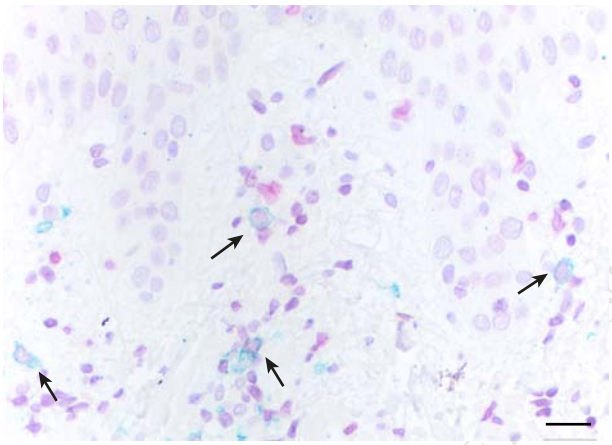

B

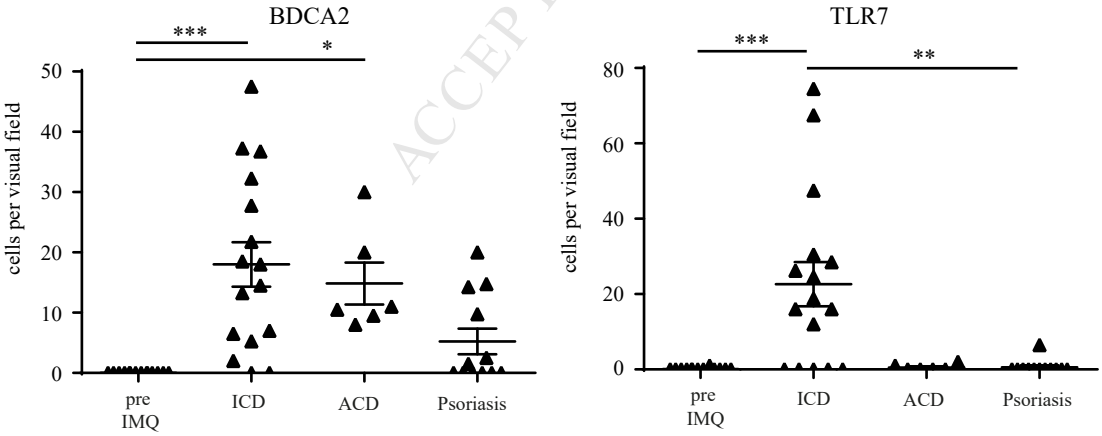

Fig. S7

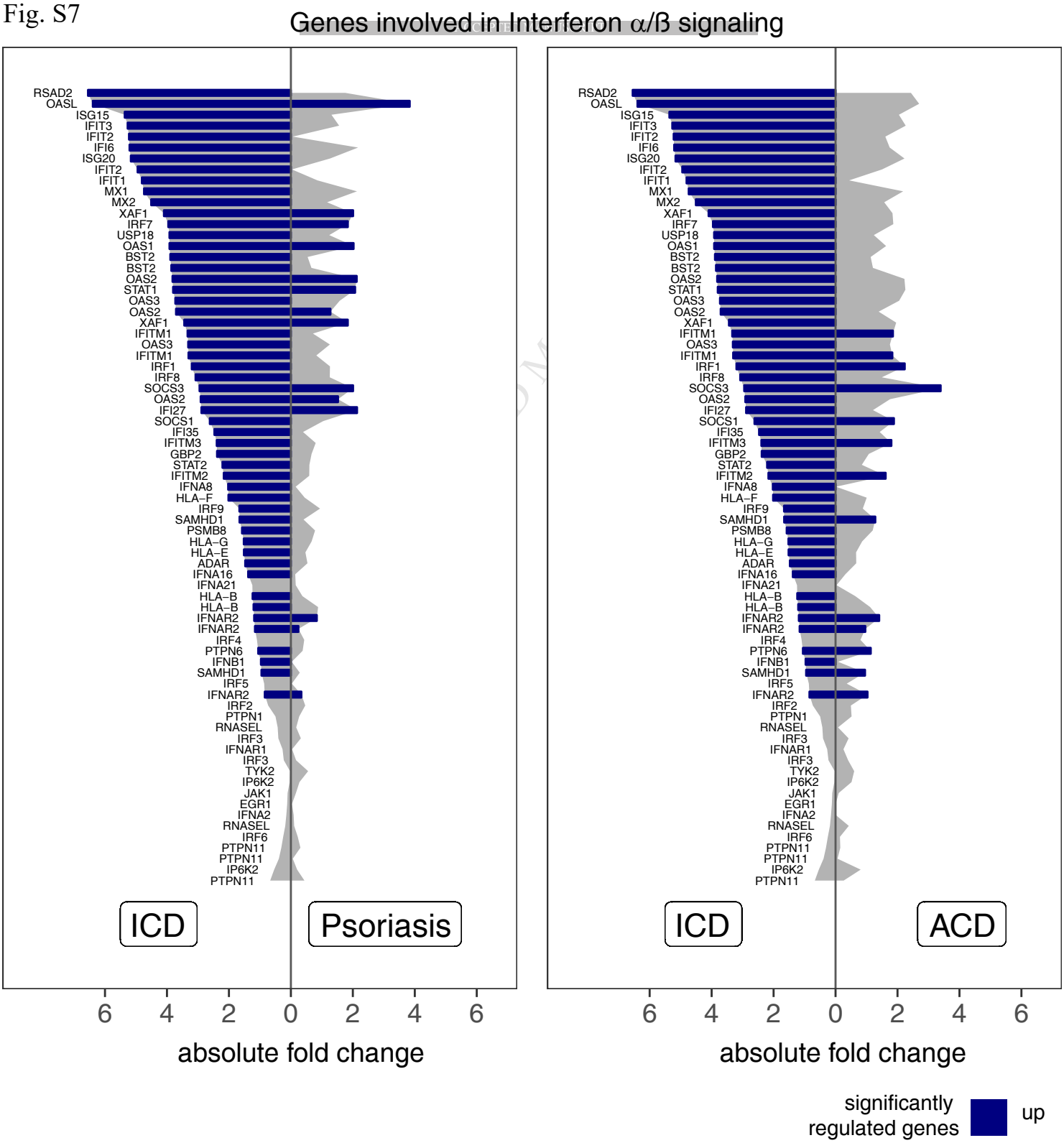
Genes involved in Interferon α/ß signaling
RSAD2
OASL
ISG15
IFIT3
IFIT2
IFI6
ISG20
IFIT2
IFIT1
MX1
MX2
XAF1
IRF7
USP18
OAS1
BST2
BST2
OAS2
STAT1
OAS3
OAS2
XAF1
IFITM1
OAS3
IFITM1
IRF1
IRF8
SOCS3
OAS2
IFI27
SOCS1
IFI35
IFITM3
GBP2
STAT2
IFITM2
IFNA8
HLA–F
IRF9
SAMHD1
PSMB8
HLA–G
HLA–E
ADAR
IFNA16
IFNA21
HLA–B
HLA–B
IFNAR2
IFNAR2
IRF4
PTPN6
IFNB1
SAMHD1
IRF5
IFNAR2
IRF2
PTPN1
RNASEL
IRF3
IFNAR1
IRF3
TYK2
IP6K2
JAK1
EGR1
IFNA2
RNASEL
IRF6
PTPN11
PTPN11
IP6K2
PTPN11
ICD
Psoriasis
ICD
ACD
6 4 2 0 2 4 6
absolute fold change
6 4 2 0 2 4 6
absolute fold change
significantly regulated genes
up

Fig. S8

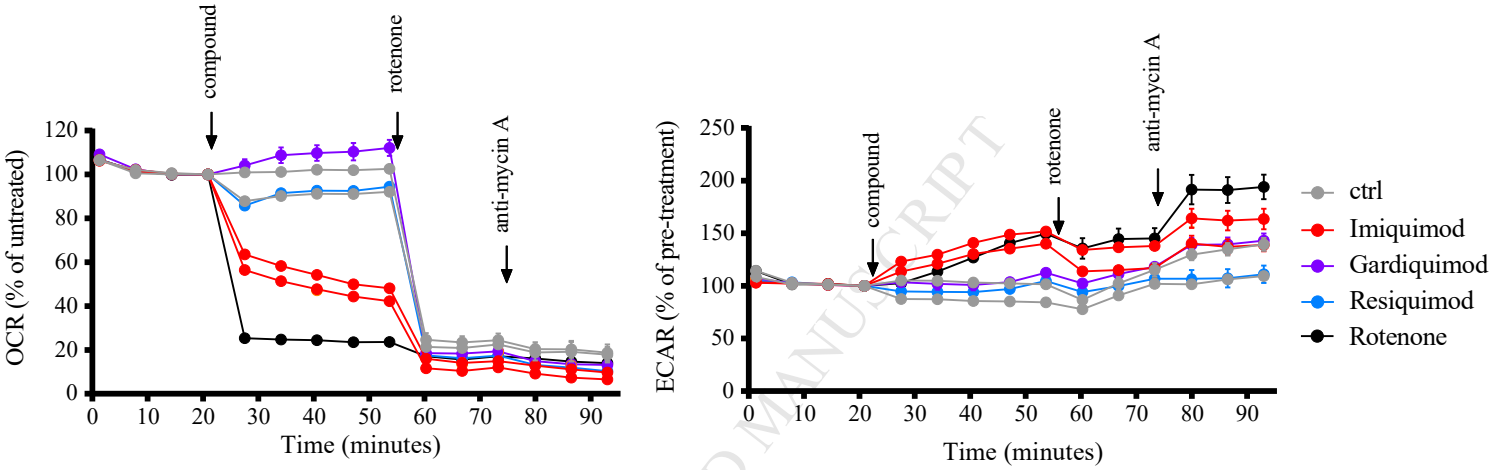

Fig. S9